Regge cuts in inclusive reactions*

Frank E. Paige and T. L. Trueman
Brookhaven National Laboratory, Upton, New York 11973
(Received 2 June 1975)

The contribution of Regge cuts to single-particle inclusive processes is analyzed using the techniques of Gribov. The dependence of these contributions on the polarization state of the target is emphasized. A general formula is obtained and certain contributions to it are calculated. It is not possible, however, to reduce this to a simple, powerful formula expressing the total cut contribution in terms of other measurable quantities, as can be done for the cut contribution to the total cross section. The reasons for this are discussed in detail. The single-particle intermediate states, analogous to the absorption model for elastic scattering, are explicitly calculated as an illustration.

I. INTRODUCTION

The Mueller-Regge analysis[1] of inclusive cross sections has had many successes. Graphs of the form shown in Fig. 1(a) seem adequate[2] to explain the unpolarized inclusive cross section for $a+b \to c+X$ in the fragmentation region of a. More specifically, graphs of the triple-Regge type, Fig. 1(b), seem adequate[3] in the region of large $s=(p_a+p_b)^2$, large $M^2=(p_a+p_b-p_c)^2$, large s/M^2, and fixed $t=(p_a-p_c)^2$. However, such graphs give no dependence on the polarization of b.[4] Such a dependence, which has recently been observed,[5] could be due to Regge-cut graphs[6,7] of the type shown in Fig. 2. The objective of this paper is to analyze these graphs.

Our calculation is based on the techniques developed by Gribov[8,9] and parallels to a large extent the calculation of cuts in the forward elastic amplitude.[10] Unfortunately, the results which we obtain are neither as simple nor as powerful as those for the total cross sections. To explain why this is so we begin by reviewing the cut calculation for the total cross section. By analyzing various possible specific insertions for the blobs in Fig. 3(a), and, especially, by making kinematic approximations appropriate to the dominant region of integration, Gribov[8,9] showed that the cut amplitude $F_{\rm cut}(s)$ at $t=0$ is given asymptotically by

$$F_{\rm cut}(s)=\frac{i}{4s}\int\frac{d^2q}{(2\pi)^2}\int\frac{ds_1}{2\pi i}\int\frac{ds_2}{2\pi i}\,\frac{\xi^2(q_\perp^2)}{\sin^2\pi\alpha(q_\perp^2)}\,s^{2\alpha(q_\perp^2)}\times A_a(s_1,q_\perp^2)A_b(s_2,q_\perp^2)\,, \tag{1.1}$$

where $\alpha(q_\perp^2)$ is the trajectory function of the exchanged poles, assumed to be identical here,

$$\xi(q_\perp^2)=1+\tau e^{-i\pi\alpha(q_\perp^2)} \tag{1.2}$$

is the signature factor, and $q_\perp$ is the two-dimensional momentum-transfer vector orthogonal to the incoming momenta, with $q^2=q_\perp^2+O(1/s)$. The Reggeon-particle amplitudes for $\alpha(q)+a\to\alpha(q)+a$ and $\alpha(-q)+b\to\alpha(-q)+b$ are denoted by A_a and A_b. These are functions, respectively, of $s_1=(p_a+q)^2$ and $s_2=(p_b-q)^2$, having the usual left- and right-hand cuts in these variables. The integration contours go below the left-hand cuts and above the right-hand ones.

Evidently if there is sufficient convergence in s_1 and s_2, then the contours of integration can be distorted so as to express $F_{\rm cut}(s)$ in terms of the discontinuities of A_a and A_b across their right-hand cuts. (Problems connected with the convergence of the integrals are discussed in Ref. 10.) This is a powerful result because these discontinuities are directly measurable in single-particle inclusive reactions.[10,11] For example, the

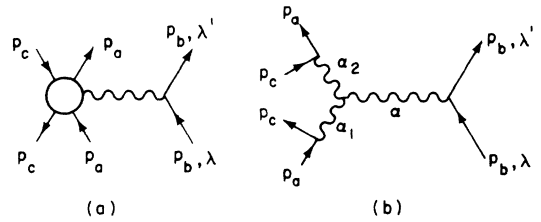

FIG. 1. (a) Mueller Regge-pole graph for inclusive cross section; (b) triple-Regge graph.

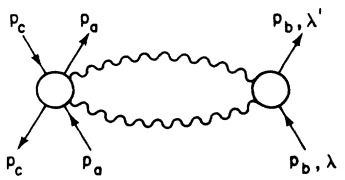

FIG. 2. Mueller Regge-cut graph.

inclusive cross section $a+b \to d+X$, e.g., Fig. 3(b), is proportional to[1,12]

$$\frac{1}{2i}\,\mathrm{disc}_{s_1} F_6 = \frac{1}{2i}\,[F_6(s+i\epsilon, \bar{s}-i\epsilon, s_1+i\epsilon, q^2) - F_6(s+i\epsilon, \bar{s}-i\epsilon, s_1-i\epsilon, q^2)], \tag{1.3}$$

where F_6 is the forward amplitude for $a+b+d \to a'+b'+\bar{d}'$ and $s=(p_a+p_b)^2$, $\bar{s}=(p_a'+p_b')^2$, $s_1=(p_a+p_b-p_d)^2$, $q^2=(p_b-p_d)^2$. (Of course, $|\bar{s}| = |s|$; these variables are distinguished because they have different boundary conditions.) In the limit $s \to \infty$ with s_1 and q^2 fixed,

$$\mathrm{disc}_{s_1} F_6 \sim \beta^2(q^2)\,\frac{s^{2\alpha(q^2)}}{\sin^2\pi\alpha(q^2)}\,\xi(q^2)\,\xi^*(q^2) \times \mathrm{disc}_{s_1} A_a(s_1, q^2)\,, \tag{1.4}$$

where A_a is the Reggeon-particle amplitude. It is readily seen that this amplitude is the same as that which enters into the calculation of $F_{\mathrm{cut}}(s)$.

The cut contribution to the total cross section is proportional to the discontinuity of $F_{\mathrm{cut}}(s)$. This can be obtained from the imaginary part, but in preparation for the more complicated problem of interest in this paper, let us calculate it directly. Properly speaking, the function given in Eq. (1.1) is $F_{\mathrm{cut}}(s+i\epsilon)$. We need to find also $F_{\mathrm{cut}}(s-i\epsilon)$. To do this we reexamine the transformation from d^4q integration associated with the Reggeon loop to the variables used in Eq. (1.1). This transformation is done by using the Sudakov parametrization[13]

$$q = xp_a + yp_b + q_\perp\,. \tag{1.5}$$

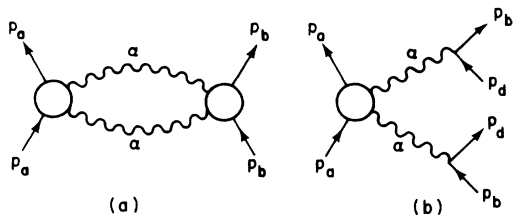

FIG. 3. (a) Regge-cut graph for total cross section; (b) related Mueller graph.

Then

$$d^4q = \tfrac{1}{2}\,[\lambda(s, m_a^2, m_b^2)]^{1/2}\,dx\,dy\,d^2q_\perp\,, \tag{1.6}$$

where

$$\lambda(a, b, c) = a^2+b^2+c^2-2ab-2bc-2ac\,. \tag{1.7}$$

We use the exact rather than the asymptotic form because we must circle the branch point of $\lambda^{1/2}$ at $s=(m_a+m_b)^2$ as well as the branch points implicit in the Reggeon signature factors in going from $s \to \infty + i\epsilon$ to $s \to \infty - i\epsilon$. The variables s_1 and s_2 are given for large s by

$$\begin{aligned} s_1 &= ys + m_a^2 + q_\perp^2\,, \\ s_2 &= -xs + m_b^2 + q_\perp^2\,. \end{aligned} \tag{1.8}$$

This shows explicitly that if s has a small imaginary part $\epsilon > 0$, then the integration contours are displaced downward for $s_i < 0$ and upward for $s_i > 0$, as earlier asserted. If $\epsilon < 0$ the opposite is true. Thus we have

$$\begin{aligned} \mathrm{disc}_s F_{\mathrm{cut}}(s) &= \frac{i}{4s}\int\frac{d^2q_\perp}{(2\pi)^2}\int_{-\infty}^{\infty}\frac{ds_1}{2\pi i}\int_{-\infty}^{\infty}\frac{ds_2}{2\pi i}\,\frac{s^{2\alpha(q_\perp^2)}}{\sin^2\pi\alpha(q_\perp^2)}\left[\xi^2(q_\perp^2)\,A_a\left(s_1+\frac{is_1}{|s_1|}\,\epsilon, q_\perp^2\right)A_b\left(s_2+\frac{is_2}{|s_2|}\,\epsilon, q_\perp^2\right)\right. \\ &\qquad \left. + \xi^{*2}(q_\perp^2)\,A_a\left(s_1-\frac{is_1}{|s_1|}\,\epsilon, q_\perp^2\right)A_b\left(s_2-\frac{is_2}{|s_2|}\,\epsilon, q_\perp^2\right)\right] \\ &= \frac{i}{4s}\int\frac{d^2q_\perp}{(2\pi)^2}\,\frac{s^{2\alpha(q_\perp^2)}}{\sin^2\pi\alpha(q_\perp^2)}\,[\xi^2(q_\perp^2)\,N_a^+(q_\perp^2)\,N_b^+(q_\perp^2) + \xi^{*2}(q_\perp^2)\,N_a^-(q_\perp^2)\,N_b^-(q_\perp^2)]\,. \end{aligned} \tag{1.9}$$

The cut coupling functions $N^\pm$ are defined by

$$N_a^\pm(q_\perp^2) = \int_{C^\pm}\frac{ds_1}{2\pi i}\,A_a(s_1, q_\perp^2)\,, \tag{1.10}$$

where the contours $C^\pm$ are as shown in Fig. 4. The sign between the two terms in Eq. (1.9) is plus rather than minus because of the branch point in Eq. (1.6).

With the strong convergence assumed by Gribov,[8,9]

$$\begin{aligned} N_a^+(q_\perp^2) &= \frac{1}{\pi}\int_{s_0}^{\infty} ds_1\,\mathrm{Im}A_a(s_1, q_\perp^2) \\ &= -N_a^-(q_\perp^2)\,. \end{aligned} \tag{1.11}$$

Hence

$$\sigma_{\text{cut}}^{\text{total}}(s) = \int \frac{d^2q_\perp}{(2\pi)^2} \frac{\cos\pi\alpha(q_\perp^2)}{\sin^2\pi\alpha(q_\perp^2)} \begin{Bmatrix} \cos^2[\frac{1}{2}\pi\alpha(q_\perp^2)] \\ -\sin^2[\frac{1}{2}\pi\alpha(q_\perp^2)] \end{Bmatrix} s^{2\alpha(q_\perp^2)-2} N_a^+(q_\perp^2) N_b^+(q_\perp^2) , \tag{1.12}$$

the upper alternative applying for $\tau = +1$, the lower for $\tau = -1$. This result of course agrees with that obtained by taking the imaginary part of Eq. (1.1) and using the optical theorem.

The above extended review is intended to make the following discussion easier to follow. At first sight one might think that the calculation of the graph in Fig. 2 would be very similar to that just outlined, and, in particular, that this graph could be calculated from the two-particle inclusive cross section, that is, from the graph shown in Fig. 5. This is not correct because the Reggeon–two-particle amplitude depends on extra variables.[14] These complicate the boundary conditions, and they also introduce extra singularities in the y Sudakov variable associated with the loop, preventing the simple contour distortion used in obtaining Eq. (1.10).

Let us first consider the two-particle inclusive cross section; cf. Fig. 5. This cross section is proportional to[1,12]

$$\frac{1}{2i}\,\text{disc}_{s'} F_8 = \frac{1}{2i}\left[F_8(s+i\epsilon, \bar{s}-i\epsilon, s_1+i\epsilon, \bar{s}_1-i\epsilon, s_2+i\epsilon, \bar{s}_2-i\epsilon, s'+i\epsilon) \right.$$
$$\left. - F_8(s+i\epsilon, \bar{s}-i\epsilon, s_1+i\epsilon, \bar{s}_1-i\epsilon, s_2+i\epsilon, \bar{s}_2-i\epsilon, s'-i\epsilon)\right] , \tag{1.13}$$

where F_8 is the forward amplitude for $a+b+\bar{c}+\bar{d} \to a'+b'+\bar{c}'+\bar{d}'$, and where

$$\begin{aligned} s &= (p_a+p_b)^2 , & \bar{s} &= (p_a'+p_b')^2 , \\ s_1 &= (p_a+p_b-p_d)^2 , & \bar{s}_1 &= (p_a'+p_b'-p_d')^2 , \\ s_2 &= (p_a+p_b-p_c)^2 , & \bar{s}_2 &= (p_a'+p_b'-p_c') , \\ s' &= (p_a+p_b-p_c-p_d)^2 . \end{aligned} \tag{1.14}$$

Momentum-transfer arguments are suppressed. As in Eq. (1.3), $|\bar{s}| = |s|$, etc. In the Regge limit appropriate for Fig. 5, $s \to \infty$, $s_2 \to \infty$, s/s_2 fixed,

$$F_8(s+i\epsilon, \bar{s}-i\epsilon, s_1+i\epsilon, \bar{s}_1-i\epsilon, s_2+i\epsilon, \bar{s}_2-i\epsilon, s'\pm i\epsilon) \sim \frac{(s)^{\alpha_2+\alpha_4}}{\sin\pi\alpha_2 \sin\pi\alpha_4} \xi_2\xi_4^* A_{++,--}(s_1+i\epsilon, \bar{s}_1-i\epsilon, s'\pm i\epsilon, s/s_2) . \tag{1.15}$$

Subscripts are used on $A_{\rho\sigma,\bar{\rho}\bar{\sigma}}$ ($\rho, \sigma, \bar{\rho}, \bar{\sigma} = \pm 1$) to indicate that it is defined by the limit $s \to \infty + i\bar{\rho}\epsilon$, $\bar{s} \to \infty + i\bar{\rho}\epsilon$, $s_2 \to \infty + i\sigma\epsilon$, $\bar{s}_2 \to \infty + i\bar{\sigma}\epsilon$ with $\epsilon > 0$. It is important to realize that the various functions $A_{\rho\sigma,\bar{\rho}\bar{\sigma}}$ are not the same, as shall be seen later by explicit examples. The ratio s/s_2 can be expressed in terms of s_1, s', and either a Toller angle[14] or the angle between $p_{c\perp}$ and $k_\perp$, so that A depends only on internal variables.

Now consider the Reggeon–two-particle amplitude as it enters in the cut graph shown in Fig. 2. Define the variables as in Eq. (1.14) but with $p_b - p_d$ replaced by k everywhere, and note that $M^2 = s_2$. To calculate the inclusive cross section we need the cut amplitudes $F_8(s+i\epsilon, \bar{s}-i\epsilon, M^2 \pm i\epsilon)$. After introducing Sudakov variables we must do the y integration over the Reggeon–two-particle blob. If $\text{Im}s > 0$ then $s_1\,\text{Im}s_1 > 0$, and if $\text{Im}\bar{s} < 0$ then $\bar{s}_1\,\text{Im}\bar{s}_1 < 0$. Hence the y contour goes below the left-hand cut and above the right-hand cut in s_1, and the opposite for the cuts in $\bar{s}_1$. Furthermore, if $\text{Im}M^2 > 0$, then $s'\,\text{Im}s' > 0$ and the contour goes below the left-hand cut and above the right-hand cut in s'. If $\text{Im}M^2 < 0$ the opposite is true. (For further discussion see Appendix A.) Thus the cut contribution to the single-particle inclusive cross section is

$$\frac{d\sigma}{dt\,dM^2} = \left(\frac{1}{16\pi s^2}\right)\left(\frac{1}{2i}\right)\left(\frac{i}{4M^2}\right)\int \frac{d^2k_\perp}{(2\pi)^2} \frac{(M^2)^{\alpha_2(k_\perp^2)+\alpha_4(k_\perp^2)}}{\sin\pi\alpha_2 \sin\pi\alpha_4} N_b(k_\perp)$$
$$\times\left[\xi_2\xi_4 \int_{C_1^+} \frac{dy}{2\pi i} A_{++,-+}(s_1, \bar{s}_1, s', s/M^2) - \xi_2^*\xi_4^* \int_{C_1^-} \frac{dy}{2\pi i} A_{+-,--}(s_1, \bar{s}_1, s', s/M^2)\right] , \tag{1.16}$$

$$s_1 = y(s+i\epsilon) + m_a^2 + k_\perp^2 , \quad \bar{s}_1 = y(s-i\epsilon) + m_a^2 + k_\perp^2 .$$

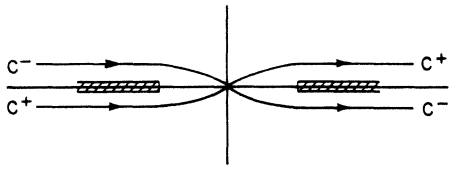

FIG. 4. Contours for Eq. (1.10).

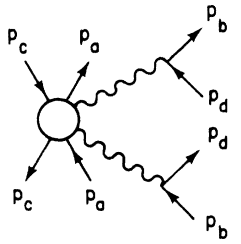

FIG. 5. Mueller graph for two-particle cross section in Regge limit.

Here s' can be expressed in terms of $s_1, s', t' = k^2 \approx k_\perp{}^2, s, M^2, t = q^2$, where $q = p_a - p_c$, and the angle φ between $q_\perp$ and $k_\perp$ by[15]

$$\frac{M^2}{s} = -\frac{\lambda^{1/2}(t, t', s')}{\lambda^{1/2}(s_1, t', m_a{}^2)} (\cos\chi + i \sin\chi \cos\varphi) , \tag{1.17}$$

with

$$\cos\chi = \frac{(t' - m_a{}^2 + s_1)(t' - s' + t) + 2t'(s' - t' + m_a{}^2 - m_b{}^2)}{\lambda^{1/2}(t', m_a{}^2, s_1)\lambda^{1/2}(t, t', s')} . \tag{1.18}$$

For this large s_1 this becomes simply

$$\frac{M^2}{s} = \frac{1}{s_1}[s' - t - t' - 2(t t')^{1/2} \cos\varphi]$$

$$= \frac{1}{s_1}[s' - (q_\perp + k_\perp)^2] . \tag{1.19}$$

Evidently a singularity of A in s' at s_0' will induce a singularity in y at a value of order s_0'/M^2. If we assume that the singularities of A are essentially those required by unitarity in s_1 and s', then the contours C_1^+ and C_1^- in Eq. (1.16) will be as shown in Fig. 6.

Thus there are two difficulties in converting Eq. (1.16) into a powerful formula like that for the total cross section in Eqs. (1.11) and (1.12). First, the Reggeon–two-particle amplitude A entering the cut calculation has different boundary conditions from that related to the two-particle inclusive cross section. Second, the singularities in s_1 prevent a distortion of the contour so that the integral cannot be expressed in terms of the discontinuity in s' which is measurable in the two-particle inclusive reaction.

These difficulties are reduced but not eliminated by considering the triple-Regge region, that is, s large, M^2 large, s/M^2 large, and $t = q^2$ fixed. In this region both the s and the s_1 dependence are, for any given graph, controlled by specified Regge poles or cuts. Thus one knows the form of the cuts in s_1, and one also knows how to change the $i\epsilon$ prescriptions. As we shall see, however, this information is not sufficient to determine completely the cut amplitudes.

For definiteness we shall assume henceforth that particles a and c have spin zero and that particle b has spin one-half. Then the cross section for $a + b \to c + X$ is related to the s-channel helicity amplitudes $F_{\lambda'\lambda}$ with Mueller boundary conditions by

$$\frac{d\sigma}{dt\, dM^2} = \frac{1}{16\pi s^2}\left[\frac{1}{2i} \operatorname{disc}_{M^2} F_{++}(s, M^2, t) - i\vec{P}_b \cdot \hat{n} \frac{1}{2i} \operatorname{disc}_{M^2} F_{-+}(s, M^2, t)\right] , \tag{1.20}$$

where $\vec{P}_b$ is the polarization vector and $\hat{n}$ is the normal to the scattering plane.

In the triple-Regge region the leading graph is the ordinary triple-Regge graph, Fig. 1(b). Its contribution to the cross section is[16]

$$\frac{d\sigma}{dt\, dM^2} = \frac{1}{16\pi s^2} \beta_{a\bar{c}}{}^2(t)\, \beta_{b\bar{b}}{}^{++}(0)\, g_{\alpha_1\alpha_3;\,\alpha}(t)\, \frac{2\,\mathrm{Re}[\xi_1(t)\xi_3^*(t)]}{\sin\pi\alpha_1(t)\sin\pi\alpha_3(t)} \left(\frac{s}{M^2}\right)^{\alpha_1(t)+\alpha_3(t)} (M^2)^{\alpha(0)} , \tag{1.21}$$

where $g_{\alpha_1\alpha_3;\,\alpha}$ is the triple-Regge coupling. As has already been noted, this graph gives no dependence on $\vec{P}_b$: The second term in Eq. (1.20) is proportional to $\beta_{-+}(0)$ and hence vanishes.

From experience with two-body amplitudes we expect that the one-loop Regge-cut graphs are the most important ones at any reasonable energy. Infinite summations of graphs[17] may be important for determining the true behavior as $\log s \to \infty$, but we will not examine that problem here. We are therefore led to consider the graphs shown in Fig. 7 together with similar ones obtained by inter-

changing the initial and the final particles. (Of course, the graph shown in Fig. 7(d) gives no dependence on $\vec{P}_b$.)

To analyze the graph in Fig. 7(a) we introduce Sudakov variables,[13]

$$k = xp_a + yp_b + k_\perp ,$$
$$q = \frac{M^2}{s} p_a + \frac{t}{s} p_b + q_\perp . \tag{1.22}$$

Then by an analysis very similar to that followed for the elastic amplitude,[8-10] we find that the dominant region of integration is $x = O(1/s)$ and $y = O(1/M^2)$. The x integral gives the Reggeon-particle vertex $N_{\alpha_4\lambda';\,\alpha_2\lambda}(k_\perp)$, where λ and λ' are the initial and final helicities. The y integral gives the four-Reggeon vertex $\Lambda_{\alpha_3\alpha_4;\,\alpha_1\alpha_2}(q_\perp, k_\perp)$. Thus the amplitude symmetrized under the interchange of α_1 and α_3 and with the Mueller boundary conditions is

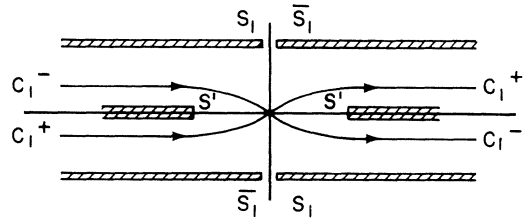

FIG. 6. Contours for Eq. (1.16). The cuts in s_i and $\bar{s}_i$ have been displaced from the real axis for clarity.

$$F_{\lambda'\lambda}(s, M^2, q^2) = \beta_1\beta_3\left(\frac{s}{M^2}\right)^{\alpha_1+\alpha_3}\left[e^{i\pi(\alpha_3-\nu_3)} + (-1)^{\lambda'-\lambda} e^{i\pi(\alpha_1-\nu_1)}\right]$$
$$\times \frac{i}{16\pi^2}\int d^2k_\perp \Lambda_{\alpha_3\alpha_4;\,\alpha_1\alpha_2}(q_\perp, k_\perp) N_{\alpha_4\lambda';\,\alpha_2\lambda}(k_\perp) e^{-i\pi(\alpha_2+\alpha_4-\nu_2-\nu_4)/2}(M^2)^{\alpha_2+\alpha_4-1}, \tag{1.23}$$

where the signature factors have been written as

$$\xi = e^{-i\pi(\alpha-\nu)/2} 2\cos\tfrac{1}{2}\pi(\alpha-\nu), \quad \nu = \tfrac{1}{2}(1-\tau) , \tag{1.24}$$

The poles associated with the Reggeons have been incorporated into Λ. The $e^{i\pi(\alpha_3-\nu_3)}$ and the $e^{i\pi(\alpha_1-\nu_1)}$ in the square brackets arise because the outgoing s and s_1 have a $-i\epsilon$ prescription,[1,12] corresponding to complex conjugation of the outgoing Reggeon's signature factor. Note that the factor in square brackets is equal to

$$e^{i\pi(\alpha_1+\alpha_3-\nu_1-\nu_3)/2} 2(i)^{\lambda'-\lambda}\cos\tfrac{1}{2}\pi(\alpha_1-\alpha_3-\nu_1+\nu_3+\lambda'-\lambda) , \tag{1.25}$$

so that the amplitude has the Regge phase associated with its M^2 behavior. The M^2 discontinuity is

$$\frac{1}{2i}\,\mathrm{disc}_{M^2} F_{\lambda'\lambda}(s, M^2, q^2) = (i)^{\lambda'-\lambda}\beta_1\beta_3\cos\tfrac{1}{2}\pi(\alpha_1-\alpha_3-\nu_1+\nu_3+\lambda'-\lambda)\left(\frac{s}{M^2}\right)^{\alpha_1+\alpha_3}$$
$$\times \frac{1}{8\pi^2}\int d^2k_\perp \Lambda_{\alpha_3\alpha_4;\,\alpha_1\alpha_2\lambda} N_{\alpha_4\lambda';\,\alpha_2\lambda}\cos\tfrac{1}{2}\pi(\alpha_1-\alpha_2+\alpha_3-\alpha_4-\nu_1+\nu_2-\nu_3+\nu_4)$$
$$\times (M^2)^{\alpha_2+\alpha_4-1}; \tag{1.26}$$

this together with Eq. (1.20) gives the cross section.

The central problem considered in Secs. III–V of this paper is the structure of Λ and the relation of it to intermediate states. Before turning to this we shall discuss the other graphs in Fig. 7.

For the graph in Fig. 7(b) the dominant region of integration is $x = O(1/s)$ and $y = O(1/s)$. If $k_i = x_i p_a + y_i p_b + k_{i\perp}$ is a momentum inside of the three-Reggeon amplitude, then the dominant region for it is $x_i = O(M^2/s)$ and $y_i = O(1/M^2)$. Thus the only x and y dependence is in the $\alpha_2 + b \to \alpha_4 + b$ and the $\alpha_2 + a \to \alpha_5 + c$ amplitudes, respectively, and these integrals give the usual N vertices. The analysis of Abramovskii, Kanchelli, and Gribov[18] shows that the only discontinuity is that through the Reggeon α_4, as can be verified by considering the $i\epsilon$ prescriptions. Thus for this graph together with the one having the initial and final particles interchanged,

$$\frac{1}{2i}\,\mathrm{disc}_{M^2} F_{\lambda'\lambda}(s, M^2, q^2) = \frac{1}{16\pi^2}\int d^2k_\perp N_{\alpha_5\alpha_2}(q + k_\perp, k_\perp) g_{\alpha_3\alpha_5;\,\alpha_4}(q_\perp, q_\perp + k_\perp)$$
$$\times N_{\alpha_4\lambda';\,\alpha_2\lambda}(k_\perp)\left[-2\,\mathrm{Im}(\xi_2\xi_5\xi_3^*)\right]\left(\frac{s}{M^2}\right)^{\alpha_2+\alpha_3+\alpha_5-1}(M^2)^{\alpha_2+\alpha_4-1} . \tag{1.27}$$

The triple-Regge vertex $g_{\alpha_3\alpha_5;\,\alpha_4}(q_\perp, q_\perp + k_\perp)$ in this formula reduces at $k_\perp = 0$ to the vertex $g_{\alpha_3\alpha_5;\,\alpha_4}(q_\perp^2)$ defined as in Eq. (1.21). The forward Reggeon-particle vertex $N_{\alpha_4\lambda';\,\alpha_2\lambda}(k_\perp)$ is given by Eq. (1.11). The

nonforward vertex $N_{\alpha_5\alpha_2}(q_\perp + k_\perp, k_\perp)$ can be studied by analyzing nonforward two-body reactions.[19] Thus by making a reasonable parametrization of the $k_\perp$ dependence of $g_{\alpha_3\alpha_5;\,\alpha_4}(q_\perp, q_\perp + k_\perp)$ it should be possible to estimate this graph. Indeed, one would expect that its size in relation to the triple-Regge graph would be comparable to the size of cuts relative to poles in two-body reactions.

For the graph in Fig. 7(c) the important region of integration is $x = O(1/s)$ and either $y = O(1/s)$ or $y = O(1/M^2)$. The calculation of the $y = O(1/s)$ regionis exactly parallel to the calculation of enhanced graphs in the elastic amplitude and gives a contribution of the same form as Eq. (1.27). In fact, the graph in Fig. 7(b) must go smoothly into that in Fig. 7(c) for large $(p_a + k)^2$. If the $N_{\alpha_5\alpha_2}$ in Eq. (1.27) is calculated by integrating the discontinuity of the Reggeon-particle amplitude over values of $(p_a + k)^2$ less than some large s_0, then the effect of including the graph in Fig. 7(a) is simply to replace $N_{\alpha_5\alpha_2}$ in Eq. (1.27) by

$$N_{\alpha_5\alpha_2}(q_\perp + k_\perp, k_\perp) - \frac{\beta_1(q_\perp^2)\, g_{\alpha_2\alpha_5;\,\alpha_1}(q_\perp + k_\perp, k_\perp)\,(s_0)^{\alpha_1 + 1 - \alpha_2 - \alpha_5}}{\alpha_1 + 1 - \alpha_2 - \alpha_5} \quad . \tag{1.28}$$

This is just the result found in Ref. 10.

The graph in Fig. 7(c) also has a contribution from $y = O(1/M^2)$ with the same form as in Eq. (1.26). In fact, the graph in Fig. 7(a) must go smoothly into that in Fig. 7(c) for y small compared to $O(1/M^2)$. This contribution is not simply related to the measured triple-Regge coupling, and a discussion of it is postponed to Sec. IV.

Finally, we consider the graph in Fig. 7(d), which contributes for $x = O(1/s)$ and either $y = O(1/M^2)$ or $y = O(1)$. The calculation of this graph is similar to that of enhanced graphs in the elastic amplitude,[10] so we only quote the result, symmetrized under the interchange of α_1 and α_3:

$$\frac{1}{2i}\,\mathrm{disc}_{M^2} F_{\lambda'\lambda}(s, M^2, q^2) = \beta_1\beta_3\,\mathrm{Re}(\xi_1\xi_3^*)\left(\frac{s}{M^2}\right)^{\alpha_1 + \alpha_3} g_{\alpha_1\alpha_3;\,\alpha_6}(q_\perp^2)$$
$$\times \frac{1}{8\pi^2}\int d^2k_\perp\, g_{\alpha_2\alpha_4;\,\alpha_6}(k_\perp^2)\, N_{\alpha_4\lambda';\,\alpha_2\lambda}(k_\perp)\left[\frac{(M^2)^{\alpha_6} - (M^2)^{\alpha_2 + \alpha_4 - 1}}{\alpha_6 + 1 - \alpha_2 - \alpha_4}\right] . \tag{1.29}$$

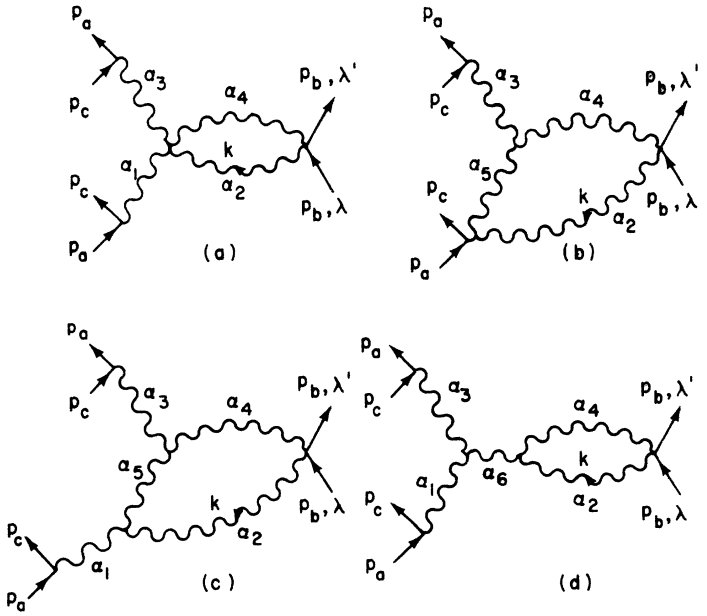

FIG. 7. Regge-cut graphs for the triple-Regge region.

Everything here is known. It is apparent from Eq. (2.13) that this amplitude vanishes for $\lambda' \neq \lambda$.

The formulas given above summarize the structure of the contributions of Regge cuts to inclusive reactions in the triple-Regge region. The outline of the remainder of this paper is as follows.

In Sec. II we give a general discussion of the effects of spin in inclusive reactions.

In Sec. III we turn to the study of the four-Reggeon vertex Λ. We consider the simplest possible model for Λ, namely the contribution of the one-particle intermediate state in $s' = (q+k)^2$. This is a natural generalization of the absorption model[19] to cuts in the Reggeon-particle amplitude, and it is closely related to a model considered recently by DeTar.[20] We find that the one-particle contribution to Λ can be expressed in terms of the double-Regge limit of the two-to-three amplitude. However, this contribution is not proportional to the two-to-three cross section. More significantly, it has singularities in the physical region.

In Sec. IV we show that these singularities are the consequence of terms in the one-particle graph with anomalous s and M^2 dependence. Such terms arise because the one-particle graph does not behave like the graphs shown in Fig. 7(c) and 7(d) in the appropriate limits. We discuss how the anomalous terms might be removed.

In Sec. V we calculate the contribution of the closed box graph to the four-Reggeon amplitude. We find that this graph has a somewhat different cut structure in s_1 than the one-particle graph, contrary to the conjecture of DeTar.[20]

In Sec. VI we give a brief summary of our results.

II. SPIN DEPENDENCE OF INCLUSIVE CROSS SECTIONS

In this section we review the properties of inclusive amplitudes associated with spin, which are needed in this paper. We assume that particle b has spin $\frac{1}{2}$ and that particles a and c have spin zero. This assumption is not important for our considerations and we make it for simplicity. The inclusive amplitude will be denoted by $F_{\lambda',\lambda}(s, M^2, t)$ where λ denotes the helicity of b in the ab center-of-mass system.

If

$$\rho_b = \tfrac{1}{2}(1 + \vec{\sigma}\cdot\vec{P}_b) \tag{2.1}$$

is the density matrix of the polarized target b in the lab frame, then the inclusive cross section is given by

$$\frac{d\sigma}{dt\,dM^2}(\vec{P}_b) = \frac{1}{16\pi s^2}\,\mathrm{disc}_{M^2} \sum_{\lambda,\lambda'} \rho_{b\lambda\lambda'} F_{\lambda',\lambda}(s, M^2, t) \ . \tag{2.2}$$

Parity invariance implies[21]

$$F_{\lambda',\lambda} = (-1)^{\lambda'-\lambda} F_{-\lambda',-\lambda} = (-1)^{\lambda'-\lambda} F_{\lambda,\lambda'} \ . \tag{2.3}$$

As a consequence

$$\frac{d\sigma}{dt\,dM^2} = \frac{1}{16\pi s^2}\left[\frac{1}{2i}\,\mathrm{disc}_{M^2} F_{++}(s, M^2, t) - i\vec{P}_b\cdot\hat{n}\frac{1}{2i}\,\mathrm{disc}_{M^2} F_{-+}(s, M^2, t)\right] \ . \tag{2.4}$$

If $\vec{p}_c$ does not lie in the x-z plane, as implicity assumed here, but has azimuthal angle φ, then the conventions of Jacob and Wick[21] imply that

$$F_{\lambda',\lambda}(s, M^2, t, \varphi) = e^{-i\varphi(\lambda'-\lambda)} F_{\lambda',\lambda}(s, M^2, t, 0) \ . \tag{2.5}$$

From the fundamental relation between the M^2 discontinuity and the sum on intermediate states it is clear that

$$\frac{1}{2i}\,\mathrm{disc}_{M^2} F_{\lambda',\lambda} = \left(\frac{1}{2i}\,\mathrm{disc}_{M^2} F_{\lambda,\lambda'}\right)^* \ . \tag{2.6}$$

Equations (2.6) and (2.3) then imply that $(1/2i)\,\mathrm{disc}_{M^2} F_{++}$ is real and $(1/2i)\,\mathrm{disc}_{M^2} F_{-+}$ is imaginary and guarantee the reality of the cross section as given by Eq. (2.4).

If we assume Regge-pole dominance of the inclusive process in the end-of-the-spectrum region, Fig. 8, $F_{\lambda',\lambda}$ has the form

$$F_{\lambda',\lambda}(s, M^2, t) = \beta_1\beta_3\xi_1\xi_3^* s^{\alpha_1(t)+\alpha_3(t)} A_{\alpha_3\lambda',\alpha_1\lambda}(M^2, t) + (1 \leftrightarrow 3) \ . \tag{2.7}$$

A is the Reggeon-particle amplitude for $\alpha_1(q) + b_\lambda \to \alpha_3(q) + b_{\lambda'}$. Time-reversal invariance can be applied to Mueller's formula[1] to reduce the expression for $d\sigma/dt\,dM^2$ in this region. We use the Jacob and Wick[21] convention

$$T|p_a p_b \lambda(+)\rangle = e^{-i\pi J_y}|p_a p_b \lambda(-)\rangle \ . \tag{2.8}$$

(Notice the change from outgoing to ingoing wave boundary conditions.) Mueller's formula then gives

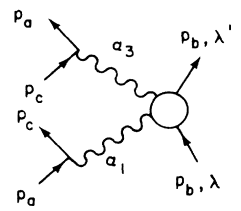

FIG. 8. Graph corresponding to Eq. (2.7).

$$\frac{1}{2i}\,\mathrm{disc}_{M^2} F_{\lambda',\lambda} = \int d^4x\, e^{-ip_c\cdot x} \langle p_a p_b \lambda'(+)|j_c(x) j_c(0)|p_a p_b \lambda(+)\rangle$$

$$= \left[\int d^4x\, e^{-ip_c\cdot x} \langle p_a p_b \lambda'(-)|j_c(x) j_c(0)|p_a p_b \lambda(-)\rangle\right]^* . \tag{2.9}$$

We assume, as usual, that in the Regge-pole-dominated amplitude, the (+) and (−) boundary conditions are interchanged by simply complex conjugating the signature factors associated with the s-dependent Regge poles. Then

$$\frac{1}{2i}\,\mathrm{disc}_{M^2} A_{\alpha_3\lambda',\alpha_1\lambda} = \left(\frac{1}{2i}\,\mathrm{disc}_{M^2} A_{\alpha_3\lambda',\alpha_1\lambda}\right)^* \tag{2.10}$$

and

$$\frac{d\sigma}{dt\,dM^2}(\vec{P}_b) \sim \frac{\beta_1\beta_3}{2\pi s^2} \cos\tfrac{1}{2}\pi(\alpha_1-\nu_1)\cos\tfrac{1}{2}\pi(\alpha_3-\nu_3)\, s^{\alpha_1+\alpha_3}$$

$$\times\Big[\cos\tfrac{1}{2}\pi(\alpha_1-\nu_1-\alpha_3+\nu_3)\,\frac{1}{2i}\,\mathrm{disc}_{M^2} A_{\alpha_3+;\alpha_1+}(M^2,t)$$

$$+\vec{n}\cdot\vec{P}_b \sin\tfrac{1}{2}\pi(\alpha_1-\nu_1-\alpha_3+\nu_3)\,\frac{1}{2i}\,\mathrm{disc}_{M^2} A_{\alpha_3-;\alpha_1+}(M^2,t)\Big] . \tag{2.11}$$

This formula takes into account all symmetrization necessary in α_1 and α_3.

In evaluating the general cut graph of the form shown in Fig. 2 it will be necessary to integrate over the transverse momentum $\vec{k}$ which we will do by integrating

$$d^2k_\perp = \tfrac{1}{2}dt'\,d\varphi ,$$

where φ is the angle between $\vec{k}_\perp$ and $\vec{p}_{c\perp}$. From (2.5) the φ dependence of the N function for the right-hand blob is trivial:

$$N_{\alpha_4\lambda',\alpha_2\lambda}(t',\varphi) = e^{-i(\lambda'-\lambda)\varphi} N_{\alpha_4\lambda',\alpha_2\lambda}(t') . \tag{2.12}$$

Similarly, from (2.3), (2.7), and (2.8)

$$N_{\alpha_4\lambda',\alpha_2\lambda} = (-1)^{\lambda'-\lambda} N_{\alpha_4-\lambda',\alpha_2-\lambda}$$

$$= (-1)^{\lambda'-\lambda} N_{\alpha_4\lambda,\alpha_2\lambda'} , \tag{2.13}$$

$$N_{\alpha_4\lambda,\alpha_2\lambda} = N_{\alpha_2\lambda,\alpha_4\lambda'} . \tag{2.14}$$

Notice that when a and c carry spin, if their helicity is not observed there is no interference between trajectories of different naturality. However, the trajectories α_2 and α_4 may in general have different naturality. If they do, Eq. (2.13) must have a minus sign on the right-hand side. In the following we assume α_2 and α_4 to have positive naturality.

The Regge-cut contribution of Fig. 7(a) [Eq. (1.23)] to $A_{\alpha_3\lambda',\alpha_1\lambda}$ is then

$$A_{\alpha_3\lambda',\alpha_1\lambda}(M^2,t) = \frac{1}{4\cos\tfrac{1}{2}\pi(\alpha_1-\nu_1)\cos\tfrac{1}{2}\pi(\alpha_3-\nu_3)}\,\frac{i}{16\pi}$$

$$\times\int_{-\infty}^{0} dt' \int_0^{2\pi}\frac{d\varphi}{2\pi}\,\Lambda_{\alpha_3\alpha_4;\alpha_1\alpha_2}(t,t',\varphi)\, e^{-i(\lambda'-\lambda)\varphi} N_{\alpha_4\lambda',\alpha_2\lambda}(t')$$

$$\times e^{-i\pi(\alpha_2+\alpha_4-\nu_2-\nu_4)/2}\, e^{i\pi(\alpha_1+\alpha_3-\nu_1-\nu_3)/2} (M^2)^{\alpha_2+\alpha_4-\alpha_1-\alpha_3-1} . \tag{2.15}$$

Notice that the explicit phase of this is just that associated with the Regge behavior in M^2. From this and Eq. (2.10) we conclude that

$$\Lambda^{(\lambda-\lambda')}_{\alpha_3\alpha_4,\alpha_1\alpha_2}(t,t') = \int_0^{2\pi}\frac{d\varphi}{2\pi}\, e^{-i(\lambda'-\lambda)\varphi}\Lambda_{\alpha_3\alpha_4;\alpha_1\alpha_2}(t,t',\varphi) \tag{2.16}$$

is real.

Thus

$$\frac{1}{2i}\,\mathrm{disc}_{M^2}A_{\alpha_3\lambda';\alpha_1\lambda}(M^2,t)=\frac{1}{4\cos\frac{1}{2}\pi(\alpha_1-\nu_1)\cos\frac{1}{2}\pi(\alpha_3-\nu_3)}$$

$$\times\frac{1}{16\pi}\int_{-\infty}^{0}dt'\,\Lambda^{(\lambda'-\lambda)}_{\alpha_3\alpha_4;\alpha_1\alpha_2}(t,t')$$

$$\times N_{\alpha_4\lambda';\alpha_2\lambda}(t')\cos\tfrac{1}{2}\pi(\alpha_1-\nu_1-\alpha_2+\nu_2+\alpha_3-\nu_3-\alpha_4+\nu_4)\,(M^2)^{\alpha_2+\alpha_4-\alpha_1-\alpha_3-1}\,. \tag{2.17}$$

III. ONE-PARTICLE GRAPHS FOR FOUR-REGGEON VERTEX

In the Introduction we found that the essential problem is calculating Regge cuts for inclusive reactions in the triple-Regge region is to determine the four-Reggeon vertex Λ. In this section we consider the simplest contribution to Λ, namely that from the one-particle graphs shown in Fig. 9. These graphs give an unsymmetrized Reggeon-particle amplitude, from which the cross section is computed by using Eq. (2.11). While Λ can be expressed in terms of the amplitudes for the appropriate double-Regge graphs, e.g., Fig. 10, it cannot be determined from the two-to-three cross section. This illustrates the general discussion in the Introduction. The double-Regge amplitude consists of two terms with different analytic structures,[22] and the cross section determines only a certain combination of them. The residue of the pole in $s'=(q+k)^2$ in the cut calculation is given by a different combination because of the Mueller $i\epsilon$ prescription, and the discontinuity of the cut in $s_1=(p_a+k)^2$ is given by just one of the terms.

The meaning of the graphs shown in Fig. 9 perhaps requires some discussion. It is well known that the graph shown in Fig. 11 does not contribute to the cut in the elastic amplitude.[8] On the other hand, the sum rule Eq. (1.11) for the Reggeon-particle vertex N certainly includes the one-particle intermediate state. The resolution[8] of this apparent contradiction is that there are multiparticle intermediate states within the Reggeon couplings. The contribution of these cancels that of the one-particle state for this particular graph but not in general. In the special case that the s' channel $(\alpha_1+a-\alpha_2+a)$ and the u' channel $(\alpha_2+a-\alpha_1+a)$ are identical, the correct one-particle contribution to N can be obtained by keeping just the s'- and u'-channel poles.

The interpretation of the graphs in Fig. 9 is similar although slightly more complicated. We shall see that for each graph there is one term for which the integration over the y Sudakov parameter, cf. Eq. (1.16), picks up only singularities in $s'=(q+k)^2$. This integral thus has the same form as that for the elastic amplitude, and the one-particle approximation is defined in a similar way. The y integration for the remaining terms picks up left-hand and right-hand singularities in $s_1=(p_a+k)^2$ as well as singularities in s'.

The one-particle graphs for the four-Reggeon vertex are evidently closely related to the double-Regge graph, Fig. 10. The amplitude for this graph consists of two terms and is conveniently written as[22-24]

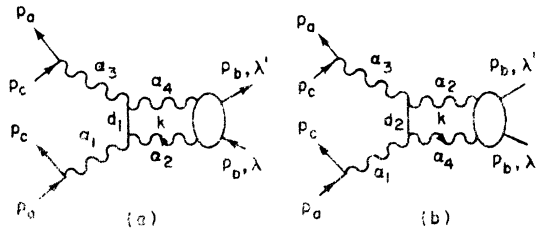

FIG. 9. One-particle graphs for four-Reggeon vertex.

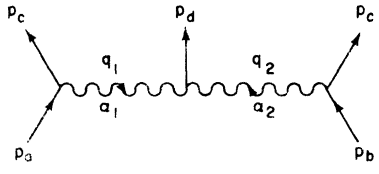

FIG. 10. Double-Regge graph.

$$F_{12}(s,s_1,s_2,t_1,t_2)=\beta_1(t_1)\,\beta_2(t_2)\left(\frac{s}{s_2}\right)^{\alpha_1(t_1)}(s_2)^{\alpha_2(t_2)}\,e^{-i\pi[\alpha_2(t_2)-\nu_2]/2}$$
$$\times[V_{12}(t_1,t_2,\eta)+e^{-i\pi[\alpha_1(t_1)-\alpha_2(t_2)-\nu_{12}]/2}\,\eta^{\alpha_1(t_1)-\alpha_2(t_2)}V_{21}(t_1,t_2,\eta)]\ , \tag{3.1}$$

where in terms of the momenta defined in Fig. 10

$$s=(p_a+p_b)^2,\quad s_1=(p_c+p_d)^2,\quad s_2=(p_d+p_e)^2,\quad t_1=q_1^{\,2},\quad t_2=q_2^{\,2},\quad \eta=m_d^{\,2}-(q_{1\perp}+q_{2\perp})^2\sim s_1s_2/s\ , \tag{3.2}$$

and where $\nu_i=\frac{1}{2}(1-\tau_i)$, $\nu_{12}=\frac{1}{2}(1-\tau_1\tau_2)$. Near $\eta=0$, V_{12} and V_{21} are analytic in η, so the two terms in Eq. (3.1) have cuts in s and s_2 and in s and s_1, respectively.[22] At right-signature points, V_{12} has poles in $\alpha_1(t_1)-\alpha_2(t_2)$; these last cancel in the full amplitude. Equation (3.1) remains valid even for $s'=(q_1+q_2)^2\neq m_d^{\,2}$, with η being replaced by $\eta'=s'-(q_{1\perp}+q_{2\perp})^2$.[23] Of course, then V_{12} and V_{21} depend on both s' and η'.

An equivalent form for F_{12} which displays more clearly the analytic structure is

$$F_{12}=\beta_1\beta_2\frac{[(s-i\epsilon)^{\alpha_1}+\tau_1(-s-i\epsilon)^{\alpha_1}][(s_2-i\epsilon)^{\alpha_2-\alpha_1}+\tau_1\tau_2(-s_2-i\epsilon)^{\alpha_2-\alpha_1}]}{4\cos\frac{1}{2}\pi(\alpha_1-\nu_1)\cos\frac{1}{2}\pi(\alpha_2-\alpha_1-\nu_{12})}\,e^{-i\pi(\nu_1-\nu_2+\nu_{12})/2}\,V_{12}$$
$$+\beta_1\beta_2\frac{[(s-i\epsilon)^{\alpha_2}+\tau_2(-s-i\epsilon)^{\alpha_2}][(s_1-i\epsilon)^{\alpha_1-\alpha_2}+\tau_1\tau_2(-s_1-i\epsilon)^{\alpha_1-\alpha_2}]}{4\cos\frac{1}{2}\pi(\alpha_2-\nu_2)\cos\frac{1}{2}\pi(\alpha_1-\alpha_2-\nu_{12})}\,V_{21}\ , \tag{3.3}$$

where it should be noted that

$$e^{-i\pi(\nu_1-\nu_2+\nu_{12})/2}=1-\tfrac{1}{2}(1-\tau_1)(1+\tau_2)=\pm1\ . \tag{3.4}$$

This rather unsymmetrical factor is introduced to simplify subsequent equations.

Since the Reggeon-particle amplitude with Mueller boundary conditions has normal analytic structure, it should have the standard Regge phase for its M^2 dependence. We can therefore calculate the amplitude and obtain the M^2 discontinuity from Eq. (2.17). For the graph shown in Fig. 9(a) with the Mueller boundary conditions[1,12]

$$F_{\lambda'\lambda}(s,M^2,t)=-i\int\frac{d^4k}{(2\pi)^4}\,\frac{1}{s'-m_1^{\,2}+i\epsilon}\,F_{12}(s,s_1,M^2,t,t')\,F_{34}(\bar s,\bar s_1,M^2,t,t')\,T_{\alpha_4\lambda';\alpha_2\lambda}(u_r)\ . \tag{3.5}$$

Here F_{12} and F_{34} are the double-Regge amplitudes for producing particle α_1, $T_{\alpha_4\lambda';\alpha_2\lambda}$ is the amplitude for the right-hand side of the graph, and

$$s=(p_a+p_b)^2,\ M^2=(p_a+p_b-p_c)^2,\ t=(p_a-p_c)^2=q^2\ ,$$
$$s_1=(p_a+k)^2,\ s'=(q+k)^2,\ u_r=(p_b-k)^2,\ t'=k^2\ . \tag{3.6}$$

A bar over any variable is used to indicate that it has a reversed $i\epsilon$ prescription, viz.,

$$s=s_r+i\frac{s_r}{|s_r|}\epsilon,\quad \bar s=s_r-i\frac{s_r}{|s_r|}\epsilon\quad (s_r=\mathrm{Res})\ . \tag{3.7}$$

Since the intermediate particle is off shell, the η variable of the double-Regge amplitudes is replaced by

$$\eta'=s'-(q_\perp+k_\perp)^2\ . \tag{3.8}$$

For the graph shown in Fig. 9(b) the amplitude is

$$F_{\lambda'\lambda}(s,M^2,t)=-i\int\frac{d^4k}{(2\pi)^4}\,\frac{1}{u'-m_2^{\,2}+i\epsilon}\,F_{14}(s,u_1,M^2,t,t')\,F_{32}(\bar s,\bar u_1,M^2,t,t')\,T_{\alpha_2\lambda';\alpha_4\lambda}(s_r)\ , \tag{3.9}$$

where F_{14} and F_{32} are double-Regge amplitudes for producing particle d_2, and

$$u_1=(p_a-k)^2\sim-s_1,\quad u'=(q-k)^2=-\eta'+(q_\perp-k_\perp)^2,\quad s_r=(p_b+k)^2\ . \tag{3.10}$$

Note that it is $V_{ij}(-\eta')$ which enters in this formula.

To analyze the integrals in Eq. (3.5) and Eq. (3.9) we introduced the scaled Sudakov[13] parametrization

$$k=\frac{1}{s}\,x'p_a+\frac{1}{M^2}\,y'p_b+k_\perp,\quad d^4k=\frac{1}{2M^2}\,dx'\,dy'\,d^2k_\perp\ . \tag{3.11}$$

By the usual arguments[8]

$$t'=k^2\approx k_\perp^{\,2}\ . \tag{3.12}$$

To leading order the only x' dependence is in $T_{\alpha_4\lambda',\alpha_2\lambda}$, and the x' integral of $\beta_2\beta_4T_{\alpha_4\lambda';\alpha_2\lambda}$ gives $N_{\alpha_4\lambda';\alpha_2\lambda}$.

For $s>0$ and $M^2>0$ we have

$$s'=y'+(q_\perp+k_\perp)^2,\quad u'=-y'+(q_\perp-k_\perp)^2,\quad s_1=\frac{s}{M^2}\,y',\quad u_1=-\frac{s}{M^2}\,y',\quad \eta'=y'\ . \tag{3.13}$$

We then find using Eq. (3.3) that the four double-Regge amplitudes appearing in Eq. (3.5) and Eq. (3.9) become

$$F_{12}=\beta_1\beta_2(s)^{\alpha_1}(M^2)^{\alpha_2-\alpha_1}e^{-i\pi(\alpha_2-\nu_2)/2}\left[V_{12}(\eta')+\frac{(\eta'-i\epsilon)^{\alpha_1-\alpha_2}+\tau_1\tau_2(-\eta'-i\epsilon)^{\alpha_1-\alpha_2}}{2\cos\frac{1}{2}\pi(\alpha_1-\alpha_2-\nu_{12})}\,V_{21}(\eta')\right],$$

$$F_{34}=\beta_3\beta_4(s)^{\alpha_3}(M^2)^{\alpha_4-\alpha_3}e^{i\pi(\alpha_3-\nu_3)}e^{-i\pi(\alpha_4-\nu_4)/2}\left[V_{34}(\eta')+\frac{(\eta'-i\epsilon)^{\alpha_3-\alpha_4}+\tau_3\tau_4(-\eta'-i\epsilon)^{\alpha_3-\alpha_4}}{2\cos\frac{1}{2}\pi(\alpha_3-\alpha_4-\nu_{34})}\,V_{43}(\eta')\right]$$

$$F_{14}=\beta_1\beta_4(s)^{\alpha_1}(M^2)^{\alpha_4-\alpha_1}e^{-i\pi(\alpha_4-\nu_4)/2}$$
$$\times\left[V_{14}(-\eta')+\frac{(\eta'-i\epsilon)^{\alpha_1-\alpha_4}+\tau_1\tau_4(-\eta'-i\epsilon)^{\alpha_1-\alpha_4}}{2\cos\frac{1}{2}\pi(\alpha_1-\alpha_4-\nu_{14})}\,\tau_1\tau_4V_{41}(-\eta')\right],$$

$$F_{32}=\beta_3\beta_2(s)^{\alpha_3}(M^2)^{\alpha_2-\alpha_3}e^{i\pi(\alpha_3-\nu_3)}e^{-i\pi(\alpha_2-\nu_2)/2}$$
$$\times\left[V_{32}(-\eta')+\frac{(\eta'-i\epsilon)^{\alpha_3-\alpha_2}+\tau_2\tau_3(-\eta'-\epsilon)^{\alpha_3-\alpha_2}}{2\cos\frac{1}{2}\pi(\alpha_3-\alpha_2-\nu_{23})}\,\tau_2\tau_3V_{23}(-\eta')\right]. \tag{3.14}$$

Making use of the formulas in Sec. II, we find after some straightforward algebra that the Reggeon-particle amplitude for these graphs has the form given in Eq. (2.15) and (2.16), with

$$\Lambda^{(\lambda'-\lambda)}_{\alpha_3\alpha_4;\,\alpha_1\alpha_2}(t,t')$$
$$=\int_0^{2\pi}\frac{d\varphi}{2\pi}\,e^{-i(\lambda'-\lambda)\varphi}$$
$$\times\int_{-\infty}^{\infty}\frac{dy'}{2\pi i}\Bigg\{\frac{1}{m_1^2-s'-i\epsilon}\Bigg[V_{12}(\eta')V_{34}(\eta')+\frac{(\eta'-i\epsilon)^{\alpha_1-\alpha_2}+\tau_1\tau_2(-\eta'-i\epsilon)^{\alpha_1-\alpha_2}}{2\cos\frac{1}{2}\pi(\alpha_1-\alpha_2-\nu_{12})}\,V_{21}(\eta')V_{34}(\eta')$$
$$+\frac{(\eta'-i\epsilon)^{\alpha_3-\alpha_4}+\tau_3\tau_4(-\eta'-i\epsilon)^{\alpha_3-\alpha_4}}{2\cos\frac{1}{2}\pi(\alpha_3-\alpha_4-\nu_{34})}\,V_{12}(\eta')V_{43}(\eta')$$
$$+\frac{(\eta'-i\epsilon)^{\alpha_1-\alpha_2+\alpha_3-\alpha_4}+\tau_1\tau_2\tau_3\tau_4(-\eta'-i\epsilon)^{\alpha_1-\alpha_2+\alpha_3-\alpha_4}}{2\cos\frac{1}{2}\pi(\alpha_1-\alpha_2+\alpha_3-\alpha_4-\nu_{12}-\nu_{34})}\,V_{21}(\eta')V_{43}(\eta')\Bigg]$$
$$+(-1)^{\lambda'-\lambda}\frac{1}{m_2^2-u'-i\epsilon}\Bigg[V_{32}(-\eta')V_{14}(-\eta')\cdot$$
$$+\frac{(\eta'-\epsilon)^{\alpha_3-\alpha_2}+\tau_2\tau_3(-\eta'-i\epsilon)^{\alpha_3-\alpha_2}}{2\cos\frac{1}{2}\pi(\alpha_3-\alpha_2-\nu_{23})}\,\tau_2\tau_3V_{23}(-\eta')V_{14}(-\eta')$$
$$+\frac{(\eta'-i\epsilon)^{\alpha_1-\alpha_4}+\tau_1\tau_4(-\eta'-i\epsilon)^{\alpha_1-\alpha_4}}{2\cos\frac{1}{2}\pi(\alpha_1-\alpha_4-\nu_{14})}\,\tau_1\tau_4V_{32}(-\eta')V_{41}(-\eta')$$
$$+\frac{(\eta'-i\epsilon)^{\alpha_1-\alpha_2+\alpha_3-\alpha_4}+\tau_1\tau_2\tau_3\tau_4(-\eta'-i\epsilon)^{\alpha_1-\alpha_2+\alpha_3-\alpha_4}}{2\cos\frac{1}{2}\pi(\alpha_1-\alpha_2+\alpha_3-\alpha_4-\nu_{23}-\nu_{14})}$$
$$\times\tau_1\tau_2\tau_3\tau_4V_{23}(-\eta')V_{41}(-\eta')\Bigg]\Bigg\}. \tag{3.15}$$

Note that from Eq. (3.14) the terms proportional to $V_{21}V_{43}$ and to $V_{23}V_{41}$ contain a product of branch points, which have been combined here.

The crucial step in this calculation is Eq. (3.14). The explicit phases in these formulas combine with the external signature factors to produce the standard Regge phase in Eq. (2.15). The y' contour for the remaining integral goes below the left-hand singularities and above the right-hand ones, and the resulting Λ is therefore real. It

is also worth noting that the product of F_{12} and F_{34} in Eq. (3.14), and hence the residue of the s' pole in the cut calculation, is not simply related to the cross section.

To do the y' integration in Eq. (3.15), we make the change of variables $\varphi \to \varphi + \pi$ for the u' terms. Using Eq. (3.13) we then have

$$\frac{1}{m_1^2 - s' - i\epsilon} \to \frac{1}{\eta_1 - y' - i\epsilon}, \quad \eta_1 = m_1^2 - (q_\perp + k_\perp)^2,$$
$$\frac{(-1)^{\lambda'-\lambda}}{m_2^2 - u' - i\epsilon} \to \frac{1}{\eta_2 + y' - i\epsilon}, \quad \eta_2 = m_2^2 - (q_\perp + k_\perp)^2. \tag{3.16}$$

In the one-particle approximation we are to ignore the s' dependence of the V_{ij}, since this comes from the effects of higher intermediate states in s'. We therefore evaluate the V_{ij} at the poles, obtaining $V_{ij}(\eta_1)$ for the s' pole terms and $V_{ij}(\eta_2)$ for the u' pole terms. However, we must not evaluate the factors of $(\eta' - i\epsilon)^{\alpha_1 - \alpha_2}$, etc., at the poles, since these factors come from cuts in s_1. If we were to do so, we would be changing the $i\epsilon$ prescription of the s_1 cuts, and we would not obtain a real cross section.

With these approximations the integral of the

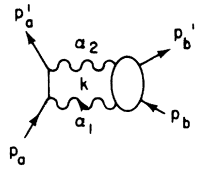

FIG. 11. Feynman graph which does not contribute to Regge cut.

s' pole term involving $V_{12}V_{34}$ is not convergent; nor is the integral of the u' pole term involving $V_{32}V_{14}$. These are the terms having poles in both α_1 and α_3, and their structure is the same as that found in calculating cuts in the elastic amplitude. In the special case that the s' and u' channels are identical, the integral over the sum of these two terms is convergent and is given by

$$\tfrac{1}{2}[\, V_{12}(\eta_1)V_{34}(\eta_1) + V_{32}(\eta_2)V_{14}(\eta_2)]. \tag{3.17}$$

We shall use this as a formal definition of the integral of these terms. The integrals of the remaining terms are all convergent for appropriate values of the α_i and can be easily evaluated. The result is

$$\begin{aligned}
\Lambda^{(\lambda'-\lambda)}_{\alpha_3\alpha_4;\alpha_1\alpha_2}(t,t') = \tfrac{1}{2}\int_0^{2\pi}\frac{d\varphi}{2\pi}\, e^{-i(\lambda'-\lambda)\varphi}\Big\{ & V_{12}(\eta_1)V_{34}(\eta_1) + \frac{1}{\cos\frac{1}{2}\pi(\alpha_1-\alpha_2-\nu_{12})}(\eta_1)^{\alpha_1-\alpha_2}V_{21}(\eta_1)V_{34}(\eta_1) \\
& + \frac{1}{\cos\frac{1}{2}\pi(\alpha_3-\alpha_4-\nu_{34})}(\eta_1)^{\alpha_3-\alpha_4}V_{12}(\eta_1)V_{43}(\eta_1) \\
& + \frac{1}{\cos\frac{1}{2}\pi(\alpha_1-\alpha_2+\alpha_3-\alpha_4-\nu_{12}-\nu_{34})}(\eta_1)^{\alpha_1-\alpha_2+\alpha_3-\alpha_4}V_{21}(\eta_1)V_{43}(\eta_1) \\
& + V_{32}(\eta_2)V_{14}(\eta_2) + \frac{1}{\cos\frac{1}{2}\pi(\alpha_3-\alpha_2-\nu_{23})}(\eta_2)^{\alpha_3-\alpha_2}V_{23}(\eta_2)V_{14}(\eta_2) \\
& + \frac{1}{\cos\frac{1}{2}\pi(\alpha_1-\alpha_4-\nu_{14})}(\eta_2)^{\alpha_1-\alpha_4}V_{32}(\eta_2)V_{41}(\eta_2) \\
& + \frac{1}{\cos\frac{1}{2}\pi(\alpha_1-\alpha_2+\alpha_3-\alpha_4-\nu_{23}-\nu_{14})}(\eta_2)^{\alpha_1-\alpha_2+\alpha_3-\alpha_4}V_{23}(\eta_2)V_{41}(\eta_2)\Big\}.
\end{aligned} \tag{3.18}$$

This is the final result for the one-particle contribution to the four-Reggeon vertex. We could evaluate this expression if we knew the amplitudes for $a+b \to c+d_{1,2}+e$, but we cannot do so from knowledge of just the corresponding cross sections. As can be seen from Eq. (3.1), the terms in the cross sections which behave like $(s)^{\alpha_1+\alpha_3}(s_2)^{\alpha_2+\alpha_4-\alpha_1-\alpha_3}$ involve the same combinations of the V_{ij}, but the cosine factors weighting them are different except for special values of the α_i. See Appendix B. This is, of course, what we expected.

For the Reggeon-particle vertex the one-particle approximation causes no difficulty and indeed is quite successful phenomenologically. The one-particle approximation for the four-Reggeon vertex has singularities for certain values of the α_i in the physical region coming from the explicit cosine factors in Eq. (3.18). Those from the $[\cos\frac{1}{2}\pi(\alpha_1-\alpha_2+\alpha_3-\alpha_4-\nu_{12}-\nu_{34})]^{-1}$ and from the $[\cos\frac{1}{2}\pi(\alpha_1-\alpha_2+\alpha_3-\alpha_4-\nu_{23}-\nu_{14})]^{-1}$ are removed when the M^2 discontinuity is taken, but the others remain. (There are, in general, no factors in the V_{ij} which cancel them.) We shall see in the next section that these singularities are reflections of additional terms with anomalous s and M^2 de-

pendence.

In the discussion following Eq. (3.1) we noted that the V_{ij} have poles in α_i-α_j which cancel in the double-Regge amplitude. They also cancel in Eq. (3.18).

IV. SINGULARITIES OF ONE-PARTICLE GRAPHS

At the end of the last section we noted that the one-particle contribution to the four-Reggeon vertex Λ has singularities as a function of t and t' in the physical region. These singularities, which are not present in the integrand in Eq. (3.15), arise from divergence of the y' integral at zero or infinity. Of course, they cannot be present in the full amplitude. In this section we discuss in some detail how they are removed. In so doing we find limits on the possible validity of a one-particle approximation for Λ, and we demonstrate the necessity of a close interrelationship among the graphs shown in Fig. 7. For definiteness we concentrate on the term in Eq. (3.18) proportional to $V_{21}(\eta)V_{34}(\eta)$, this being singular at

$$\alpha_1 - \alpha_2 = 2n + 1 + \nu_{12}, \quad n = 0, \pm 1, \pm 2, \ldots . \tag{4.1}$$

We should check our previous assertion that $V_{21}(\eta)$ does not have zeros at these points. For simplicity we assume that all of the trajectories have positive signature. We first consider the case in which there are no fixed poles. Then the form of V_{21} is[24]

$$V_{21}(\eta) = 4\cos\tfrac{1}{2}\pi\alpha_2 \cos\tfrac{1}{2}\pi(\alpha_1 - \alpha_2) \times \sum_{i=0}^{\infty} \Gamma(-\alpha_2 + i)\Gamma(\alpha_2 - \alpha_1 - i) v_i \frac{\eta^i}{i!}, \tag{4.2}$$

where the v_i are arbitrary functions of the momentum transfers. Evidently V_{21} does not in general vanish at any of the values of $\alpha_1 - \alpha_2$ in Eq. (4.1). However, as $\eta \to 0$,

$$V_{21}(\eta) \sim (\eta)^{-2n-1}, \quad \alpha_1 - \alpha_2 = 2n + 1 < 0. \tag{4.3}$$

Had we not ignored the η' dependence of V_{21} in Eq. (3.15), this behavior would make the y' integral convergent at zero, thus eliminating the singularities at negative values of $\alpha_1 - \alpha_2$.

We now consider the case in which there is a multiplicative fixed pole at $j_1 - m = -1$, j_1 being the angular momentum for α_1 and m being the helicity for the two-Reggeon-particle vertex.[24] Such fixed poles are present in nonplanar graphs.[25] Then the form of V_{21} is

$$V_{21}(\eta) = 4\cos\tfrac{1}{2}\pi\alpha_2 \cos\tfrac{1}{2}\pi(\alpha_1 - \alpha_2) \times \sum_{i=0}^{\infty} \frac{\Gamma(-\alpha_2 + 1)\Gamma(\alpha_2 - \alpha_1 - i)}{\alpha_1 - \alpha_2 + 1 + i} v_i \frac{\eta^i}{i!} \tag{4.4}$$

so that Eq. (4.3) does not hold in this case. Thus Λ would be singular even if we kept the y' dependence of V_{21} in doing the y' integral.

The full amplitude for the one-particle graphs must, of course, be analytic even though Λ is singular. Thus, the singularities in Λ must be canceled by singularities in other terms having the same s and M^2 dependence at the singular points. This is a familiar phenomenon in the Reggeon calculus. For example, we recall that the amplitude for the graph shown in Fig. 12 is[8-10]

$$F(s,t) = \frac{1}{16\pi}\int d^2k\, \beta_{\alpha_0} g_{\alpha_1\alpha_2;\alpha_0} N_{\alpha_1\alpha_2} \times \left[\frac{e^{-i\pi(\alpha_1+\alpha_2-1)/2}(s)^{\alpha_1+\alpha_2-1}}{\alpha_0 + 1 - \alpha_1 - \alpha_2} - \frac{e^{-i\pi\alpha_0/2}(s)^{\alpha_0}}{\alpha_0 + 1 - \alpha_1 - \alpha_2}\right]. \tag{4.5}$$

The first term in square brackets is the Regge-cut term; the second, a correction to the Regge-pole term. Each term is singular at $\alpha_1 + \alpha_2 - 1 = \alpha_0$, and these singularities cancel in the full amplitude. A similar cancellation of singularities has been observed in calculations of triple-Regge graphs,[26] but this case is less interesting because only one of the terms has a discontinuity in M^2.

The singularities of Λ indicate the transitions between the dominance of the usual cut term and of other terms in the asymptotic behavior of the one-particle graphs. The extra terms come from regions of integration in which we expect the one-particle graph to be a bad approximation to the full four-Reggeon amplitude. It is nevertheless instructive to study these terms since they illustrate the nature of the problem. To do so we recall that in deriving Eq. (3.15) for the one-particle contribution to Λ, we assumed that the energies across the Reggeons are large and that the momentum transfers are small. This is true only for

$$c_1 \frac{M^2}{s} < |y'| < c_2 M^2, \tag{4.6}$$

the precise values of the constants c_1 and c_2 not being important. For larger $|y'|$, $t' = k^2$ is large

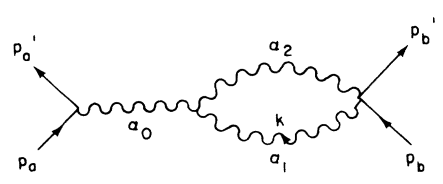

FIG. 12. Graph corresponding to Eq. (4.5).

and the integrand should be small. For smaller $|y'|$, s_1 is small and the thresholds in it must be considered. Both effects are most easily taken into account simply be restricting the y' integral in Eq. (3.15) to the domain given in Eq. (4.6). (One can check that other possible modifications of the integral give similar results.) Then in place of the $V_{21}V_{34}$ term in Eq. (3.15) we must consider

$$\tilde{\Lambda} = \int_0^{2\pi} \frac{d\varphi}{2\pi} e^{-i(\lambda'-\lambda)\varphi} V_{21}(\eta) V_{34}(\eta) \int_{c_1 M^2/s < |y'| < c_2 M^2} \frac{dy'}{2\pi i} \frac{1}{\eta - y' - i\epsilon} \frac{(y'-i\epsilon)^{\alpha_1-\alpha_2} + \tau_1\tau_2(-y'-\epsilon)^{\alpha_1-\alpha_2}}{2\cos\frac{1}{2}\pi(\alpha_1-\alpha_2-\nu_{12})} \tag{4.7}$$

We find that

$$\begin{aligned}\tilde{\Lambda} = \int_0^{2\pi} \frac{d\varphi}{2\pi} e^{-i(\lambda'-\lambda)\varphi} V_{21}(\eta)\, V_{34}(\eta) \\ \times\Bigg[\frac{(\eta)^{\alpha_1-\alpha_2}}{2\cos\frac{1}{2}\pi(\alpha_1-\alpha_2-\nu_{12})} + \frac{1}{\pi}(\eta)^{-1-\nu_{12}} \frac{e^{-i\pi(\alpha_1-\alpha_2-1-\nu_{12})/2}}{\alpha_1-\alpha_2+1+\nu_{12}} \left(c_1\frac{M^2}{s}\right)^{\alpha_1-\alpha_2+1+\nu_{12}} \\ - \frac{1}{\pi}(\eta)^{1-\nu_{12}} \frac{e^{-i\pi(\alpha_1-\alpha_2-1-\nu_{12})/2}}{\alpha_2-\alpha_1+1-\nu_{12}} \left(\frac{1}{c_2 M^2}\right)^{\alpha_2-\alpha_1+1-\nu_{12}} + \cdots\Bigg] .\end{aligned} \tag{4.8}$$

Evidently the extra terms in Eq. (4.8) are negligible for $|\alpha_1 - \alpha_2 + \nu_{12}| < 1$ but cancel the singularities of the first term at $\alpha_1 - \alpha_2 = -\nu_{12} \pm 1$. The omitted terms indicated by the three dots cancel the singularities of the first term at larger values of $|\alpha_1 - \alpha_2|$. This cancellation is guaranteed by the fact that $\tilde{\Lambda}$ is defined in Eq. (4.7) as an integral of an analytic function over a finite domain. The singular parts of the extra terms are independent of the constants c_1 and c_2, but the finite parts depend on these constants.

The first of the extra terms in Eq. (4.8) comes from small values of $|y'|$. Recalling Eq. (1.23), we see that this term gives an s and M^2 dependence of

$$(s/M^2)^{\alpha_2+\alpha_3-1-\nu_{12}} (M^2)^{\alpha_2+\alpha_4-1} . \tag{4.9}$$

Within integer powers this dependence corresponds to a Reggeon α_3 and a Reggeon (α_2)–particle cut in the $a\bar{c}$ channels and to a Reggeon (α_2)– Reggeon (α_4) cut in the $b\bar{b}$ channel. The origin of the Reggeon-particle cut can be seen by looking at Fig. 9(a). For small $|y'|$ the energy across the Reggeon α_1 is small and the dominant behavior comes from the Reggeon (α_2)–particle (d_1) cut.

The second extra term in Eq. (4.8) comes from large $|y'|$ and gives an s and M^2 dependence of

$$(s/M^2)^{\alpha_1+\alpha_3} (M^2)^{\alpha_1+\alpha_4-2+\nu_{12}} . \tag{4.10}$$

Since this term comes from a region of integration in which $s' \sim M^2$, its M^2 behavior is controlled by the large-s' behavior of the one-particle graph.

Clearly all of these extra terms are rather artificial. Consequently, a one-particle approximation for Λ, if it is valid at all, cannot be expected to be valid in the neighborhood of the singularities cancelled by these extra terms.

We wish to avoid artificial singularities in Λ and with them artificial extra terms like those in Eq. (4.8). Now, in general, Λ is related to the four-Reggeon amplitude $A_{\alpha_3\alpha_4;\alpha_1\alpha_2}$ by

$$\begin{aligned}\Lambda^{(\lambda'-\lambda)}_{\alpha_3\alpha_4;\alpha_1\alpha_2}(t,t') = \int_0^{2\pi} \frac{d\varphi}{2\pi} e^{-i(\lambda'-\lambda)\varphi} \\ \times \int_{-\infty}^{\infty} \frac{dy'}{2\pi i} A_{\alpha_3\alpha_4;\alpha_1\alpha_2}(s', \eta', t, t') ,\end{aligned} \tag{4.11}$$

$$s' = y' + (q_\perp + k_\perp)^2, \quad \eta' = y' ,$$

where the variables are defined as in Eq. (3.15) and have similar $i\epsilon$ prescriptions. We must therefore discuss the behavior of $A_{\alpha_3\alpha_4;\alpha_1\alpha_2}$ for small and large values of η'.

For small η' we have seen that the $V_{21}V_{34}$ term of the one-particle graph has an $(\eta')^{\alpha_1-\alpha_2}$ branch point, giving a singularity in Λ which must be canceled by a Reggeon-particle cut term. We do not expect Reggeon-particle cuts to be present on the physical sheet of the j plane.[27] Rather, we expect that the particle should be replaced by a Regge pole, as in the graph shown in Fig. 7(c). This graph behaves like $(\eta')^{\alpha_1-\alpha_2-\alpha_5}$ as $\eta' \to 0$, so that the y' integral in Eq. (4.11) produces a singularity at $\alpha_2 + \alpha_5 - 1 = \alpha_1$. This singularity must cancel that in $N_{\alpha_5\alpha_2}$ from the same graph, Eq. (1.28); as we have seen in the Introduction the contribution of the latter can be estimated from measurable quantities. That is, the graph shown in Fig. 7(a) must approach smoothly that shown in Fig. 7(c) for $\eta' \sim M^2/s$.

For large η', and hence large s', we expect that the four-Reggeon amplitude has Regge behavior. Since we have defined the four-Reggeon amplitude by extracting a factor of $(s/M^2)^{\alpha_1+\alpha_3}(M^2)^{\alpha_2+\alpha_4}$, the appropriate behavior is $(\eta')^{\alpha_6-\alpha_2-\alpha_4}$. Then the y' integral gives a singularity at $\alpha_2 + \alpha_1 - 1 = \alpha_6$, as

in Eq. (1.29). That is, the graph shown in Fig. 7(a) must approach smoothly that shown in Fig. 7(d) for large η'.

A similar analysis can be carried through for the $V_{21}V_{43}$ term in Eq. (3.18). The extra terms found in this case have no discontinuity in M^2, reflecting the fact that for this term the singularities of Λ are canceled by taking the M^2 discontinuity. The extra term which cancels the singularity produced by integrating the $(\eta')^{\alpha_1-\alpha_2+\alpha_3-\alpha_4}$ branch point at $\eta'=0$ behaves like $(s)^{\alpha_2+\alpha_4-1}$. It is thus the analog of the extra term found in calculations of triple-Regge graphs.[26]

It is amusing to note that the four-Reggeon amplitude for the leading trajectory in the dual model[28] has just the behavior discussed above both for $\eta'\to 0$ and for $\eta'\to\infty$. For $s'<0$ and $\eta'<0$ the amplitude is

$$A_{\alpha_3\alpha_4;\alpha_1\alpha_2}(s',\eta') = (\eta')^{\alpha_1+\alpha_3}\int_0^1 dx\,(x)^{-\alpha_6+\alpha_1+\alpha_2+\alpha_3+\alpha_4-1}(1-x)^{-\alpha_5-1}$$
$$\times\int_0^\infty dy_1\,dy_2\,dy_3\,dy_4(y_1)^{-\alpha_1-1}(y_2)^{-\alpha_2-1}(y_3)^{-\alpha_3-1}(y_4)^{-\alpha_4-1}$$
$$\times\exp\left[-y_1-y_2-y_3-y_4+\frac{(y_1y_2+y_3y_4)}{x\eta'}+\frac{(y_1y_4+y_2y_3)(1-x)}{x\eta'}\right], \tag{4.12}$$

where the first factor of $(\eta')^{\alpha_1+\alpha_3}$ reflects the fact that the four-Reggeon is defined by extracting a factor of $(s/M^2)^{\alpha_1+\alpha_3}(M^2)^{\alpha_2+\alpha_4}$. As $\eta'\to 0$ the amplitude is given by a sum of four terms with the behavior

$$(\eta')^0,\quad (\eta')^{\alpha_1-\alpha_2-\alpha_5},\quad (\eta')^{\alpha_3-\alpha_4-\alpha_5},\quad (\eta')^{\alpha_1-\alpha_2+\alpha_3-\alpha_4}. \tag{4.13}$$

As $\eta'\to-\infty$, and hence $\alpha_5\to-\infty$,

$$A_{\alpha_3\alpha_4;\alpha_1\alpha_2}\sim(-\eta')^{\alpha_6-\alpha_2-\alpha_4}. \tag{4.14}$$

Since we cannot express Λ in terms of observable quantities, we must resort to models for the four-Reggeon amplitude. Any model must provide a smooth interpolation between the poles and other singularities at finite η' and the required behavior at small and large η'. While the dual model provides one example of such a model, it is far from unique. However, by considering various models with the right properties one may be able to estimate roughly the size of Λ.

We know phenomenologically that the one-particle approximation for the Reggeon-particle vertex N is reasonably good.[10,11,19] In principle this has problems similar to those of the one-particle approximation for Λ. For N, however, the problem occurs only in the neighborhood of $j=-1$, and so is of little interest, while for Λ it can occur in interesting regions. Thus if α_1 is the f trajectory and α_2 is the Pomeron, then the first extra term in Eq. (4.8) is singular at $t\approx-0.5$ GeV^2 and $t'\approx 0$. At this point the one-particle approximation is obviously wrong.

V. CROSSED BOX GRAPH FOR FOUR-REGGEON AMPLITUDE

In calculating the one-particle graphs in Sec. III, we found that the cuts in s_1 associated with the external Reggeons are reflected in branch points at $\eta'=0$ of the four-Reggeon amplitude $A_{\alpha_3\alpha_4;\alpha_1\alpha_2}(s',\eta't,t')$. For the s' pole graph these branch points have the forms $(\eta')^0$, $(\eta')^{\alpha_1-\alpha_2}$, $(\eta')^{\alpha_3-\alpha_4}$, and $(\eta')^{\alpha_1-\alpha_2+\alpha_3-\alpha_4}$. We have seen in Sec. IV that if contributions from Reggeon-particle cuts are to be avoided, then the $(\eta')^{\alpha_1-\alpha_2}$ and the $(\eta')^{\alpha_3-\alpha_4}$ branch points must be modified. In the dual model, they are replaced by $(\eta')^{\alpha_1-\alpha_2-\alpha_5}$ and $(\eta')^{\alpha_3-\alpha_4-\alpha_5}$ branch points, solving the Reggeon-particle cut problem, but the structure is not other wise changed. One might thus be tempted to conjecture that a structure like this is in some sense general.[20]

In this section we analyze the crossed box graph, Fig. 13, for the four-Reggeon amplitude and find that its structure is somewhat different. It does have the $(\eta')^0$ and the $(\eta')^{\alpha_1-\alpha_2+\alpha_3-\alpha_4}$ branch points found previously, but it also has an $(\eta')^{\alpha_1+\alpha_3+1}$ branch point. The reason for this extra term can be understood heuristically by considering the related two-particle double-Regge graph shown in Fig. 14. Evidently this graph behaves like $(s_1')^{\alpha_1}$,

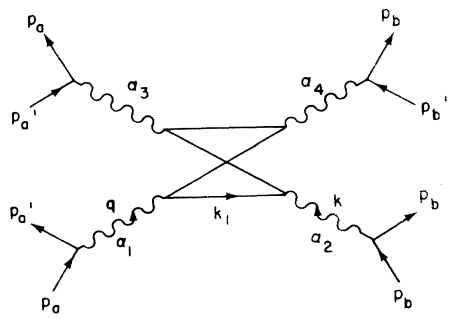

FIG. 13. Crossed box graph for four-Reggeon amplitude.

$(s_2')^{\alpha_2}$ for s, s_1, s_2, s_1', s_2' large and the other variables fixed. But in the same limit $s_1' \sim s_1$, $s_2' \sim s_2$, so the behavior of the graph is effectively

$$(s_1)^{\alpha_1}(s_2)^{\alpha_2} = (s)^{\alpha_1}(s_2)^{\alpha_2-\alpha_1}(\eta')^{\alpha_1}, \tag{5.1}$$

since $\eta' \sim s_1 s_2/s$. This $(\eta')^{\alpha_1}$ leads to the $(\eta')^{\alpha_1+\alpha_3+1}$ branch point.

We shall analyze the crossed box graph as part of the graph shown in Fig. 13 rather than as part of a cut graph. For simplicity we shall use Feynman boundary conditions and assume that all trajectories have positive signature. The variables are

$$\begin{aligned} &s=(p_a+p_b)^2,\ s_1=(p_a+k)^2,\ s_2=(p_b+q)^2,\\ &s'=(q+k)^2,\ t=q^2,\ t'=k^2,\\ &\eta'=s'-(q_\perp+k_\perp)^2 \sim s_1 s_2/s\ . \end{aligned} \tag{5.2}$$

The momenta can be parametrized as

$$\begin{aligned} &q=\frac{s_2}{s}\,p_a+\frac{t}{s}\,p_b+q_\perp,\ q^2\approx q_\perp{}^2\ ,\\ &k=\frac{t'}{s}\,p_a+\frac{s_1}{s}\,p_b+k_\perp,\ k^2\approx k_\perp{}^2,\\ &k_1=\frac{s_2}{s}\,x_1 p_a+\frac{\eta'}{s_2}\,y_1 p_b+k_{1\perp}. \end{aligned} \tag{5.3}$$

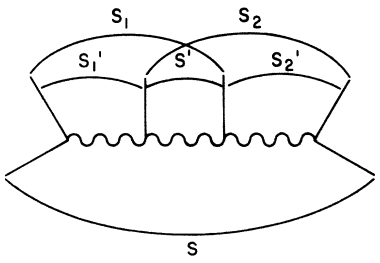

FIG. 14. Two-particle double-Regge graph.

Then with the usual approximations[8] the amplitude for the graph shown in Fig. 13 is given by

$$F=\beta_1\beta_2\beta_3\beta_4\left(\frac{s}{s_2}\right)^{\alpha_1+\alpha_3}(s_2)^{\alpha_2+\alpha_4}A_{\alpha_3\alpha_4;\alpha_1\alpha_2}(s',\eta',t,t'), \tag{5.4}$$

where $A_{\alpha_3\alpha_4;\alpha_1\alpha_2}$, which is identified as the Regge-on-particle amplitude with the same energy factors extracted as for the cut calculation, is

$$\begin{aligned} A_{\alpha_3\alpha_4;\alpha_1\alpha_2} = {}& \frac{1}{2(2\pi)^4}(\eta')^{\alpha_1+\alpha_3+1}\\ &\times\int d^2k_{1\perp}\int_{-\infty}^{\infty}dx_1dy_1[(-y_1-i\epsilon)^{\alpha_1}+(y_1-i\epsilon)^{\alpha_1}]\\ &\times[(x_1-i\epsilon)^{\alpha_2}+(-x_1-i\epsilon)^{\alpha_2}][(1+y_1-i\epsilon)^{\alpha_3}+(-1-y_1-i\epsilon)^{\alpha_3}]\\ &\times[(1-x_1-i\epsilon)^{\alpha_4}+(-1-x_1-i\epsilon)^{\alpha_4}]\\ &\times\frac{1}{x_1y_1\eta'+k_{1\perp}{}^2-m^2+i\epsilon}\ \frac{1}{x_1(1+y_1)\eta'+(k_{1\perp}+k_\perp)^2-m^2+i\epsilon}\\ &\times\frac{1}{(x_1-1)(y_1+1)\eta'+(k_{1\perp}+k_\perp-q_\perp)^2-m^2+i\epsilon}\ \frac{1}{(x_1-1)y_1\eta'+(k_{1\perp}-q_\perp)^2-m^2+i\epsilon}\ . \end{aligned} \tag{5.5}$$

The problem is to analyze the behavior of this function as $\eta' \to 0$.

We can see immediately from Eq. (5.5) that $A_{\alpha_3\alpha_4;\alpha_1\alpha_2}$ has an $(\eta')^{\alpha_1+\alpha_3+1}$ term. Setting $\eta'=0$ inside of the integral gives

$$A_{\alpha_3\alpha_4;\alpha_1\alpha_2}=\frac{1}{2(2\pi)^4}(\eta')^{\alpha_1+\alpha_3+1}\int d^2k_1\,\frac{1}{k_{1\perp}{}^2-m^2}\ \frac{1}{(k_{1\perp}+k_\perp)^2-m^2}\ \frac{1}{(k_{1\perp}+k_\perp-q_\perp)^2-m^2}\ \frac{1}{(k_{1\perp}-q_\perp)^2-m^2}\ I_{\alpha_1\alpha_3}I_{\alpha_2\alpha_4}, \tag{5.6}$$

where

$$\begin{aligned} I_{\alpha_1\alpha_3} &= \int_{-\infty}^{\infty}dy_1[(y_1-i\epsilon)^{\alpha_1}+(-y_1-i\epsilon)^{\alpha_1}][(1+y_1-i\epsilon)^{\alpha_3}+(-1-y_1-i\epsilon)^{\alpha_3}]\\ &= -4\pi e^{-i\pi(\alpha_1+\alpha_3)/2}\sin\tfrac{1}{2}\pi(\alpha_1+\alpha_3)\,\frac{\Gamma(-\alpha_1-\alpha_3-1)}{\Gamma(-\alpha_1)\Gamma(-\alpha_3)}\ . \end{aligned} \tag{5.7}$$

Evidently the integral for $I_{\alpha_1\alpha_3}$ is convergent and nonzero for

$$\alpha_1+\alpha_3<-1,\ \alpha_1>-1,\ \alpha_3>-1\,. \tag{5.8}$$

Hence in this domain $A_{\alpha_3\alpha_4;\alpha_1\alpha_2}$ behaves like $(\eta')^{\alpha_1+\alpha_3+1}$ as $\eta'\to 0$. Notice that $I_{\alpha_1\alpha_3}$ has zeros which cancel the poles (not shown explicitly) in α_1 and α_3. Similarly, $I_{\alpha_2\alpha_4}$ cancels the poles in α_2 and α_4, so the $(\eta')^{\alpha_1+\alpha_3+1}$ term has no poles.

To analyze the structure of $A_{\alpha_3\alpha_4;\alpha_1\alpha_2}$ more completely, we write the propagators in Eq. (5.5) in exponentiated form:

$$\begin{aligned}A_{\alpha_3\alpha_4;\alpha_1\alpha_2} = {}& \frac{1}{2(2\pi)^4}\,\xi_1\xi_2\xi_3\xi_4(\eta')^{\alpha_1+\alpha_3+1}\\ &\times\int_0^\infty d\lambda_1 d\lambda_2 d\lambda_3 d\lambda_4 \int d^2k_{1\perp}\int_{-\infty}^{\infty} dx_1 dy_1 |-y_1|^{\alpha_1}|x_1|^{\alpha_2}|1+y_1|^{\alpha_3}|1-x_1|^{\alpha_4}\\ &\times\exp\big(i\{\lambda_1[x_1y_1\eta'+k_{1\perp}{}^2-m^2]+\lambda_2[x_1(1+y_1)\eta'+(k_{1\perp}+k_\perp)^2-m^2]\\ &\quad+\lambda_3[(x_1-1)y_1\eta'+(k_{1\perp}-q_\perp)^2-m^2]\\ &\quad+\lambda_4[(x_1-1)(y_1+1)\eta'+(k_{1\perp}+k_\perp-q_\perp)^2-m^2]\}\big)\,.\end{aligned} \tag{5.9}$$

The integrals over $\lambda_1\cdots\lambda_4$ and $\vec{k}_1$ do not change the character of the branch points at $\eta'=0$, since this depends only on the α_i. It is therefore sufficient to consider the function

$$f(\eta')=(\eta')^{\alpha_1+\alpha_3+1}\int_{-\infty}^{\infty} dx\,dy\,|y|^{\alpha_1}|x|^{\alpha_2}|1-y|^{\alpha_3}|1-x|^{\alpha_4}\exp\{i\eta'[-\lambda_1xy+\lambda_2x(1-y)+\lambda_3(1-x)y-\lambda_4(1-x)(1-y)]\}\,. \tag{5.10}$$

The structure of this function at $\eta'=0$ is the same as that of $A_{\alpha_3\alpha_4;\alpha_1\alpha_2}$.

The y integration in Eq. (5.10) can be done in terms of confluent hypergeometric functions.[29] The result after combining terms is

$$f(\eta')=\frac{\Gamma(\alpha_1+1)\Gamma(\alpha_3+1)}{\Gamma(\alpha_1+\alpha_3+2)}\left[1-\frac{\sin\pi\alpha_1+\sin\pi\alpha_3}{\sin\pi(\alpha_1+\alpha_3)}\right]f_1(\eta')+\frac{2}{\Gamma(-\alpha_1-\alpha_3)}\sin\tfrac{1}{2}\pi(\alpha_1+\alpha_3)f_2(\eta')\,, \tag{5.11}$$

where

$$\begin{aligned}f_1(\eta') &= (\eta')^{\alpha_1+\alpha_3+1}\int_{-\infty}^{\infty} dx|x|^{\alpha_2}|1-x|^{\alpha_4}e^{i\eta'v}M(\alpha_1+1,\alpha_1+\alpha_3+2;-i\eta'u)\,,\\ f_2(\eta') &= \int_{-\infty}^{\infty} dx|x|^{\alpha_2}|1-x|^{\alpha_4}e^{i\eta'v}|u|^{-\alpha_1-\alpha_3-1}M(-\alpha_3,-\alpha_1-\alpha_3;-i\eta'u)\,,\\ u &= (\lambda_1+\lambda_2)x-(\lambda_3+\lambda_4)(1-x)\,,\quad v=\lambda_2x-\lambda_4(1-x)\,.\end{aligned} \tag{5.12}$$

We first consider $f_1(\eta')$. We take the limit $\eta'\to 0$ inside of the integral, this being legitimate provided that the resulting integral converges. Then

$$f_1(\eta')\sim(\eta')^{\alpha_1+\alpha_3+1}\int_{-\infty}^{\infty} dx|x|^{\alpha_2}|1-x|^{\alpha_4}\,. \tag{5.13}$$

This integral converges at $x=\infty$ provided that $\alpha_2+\alpha_4<-1$. Any divergence at $x=0$ or at $x=1$ results from the original integral for $f_1(\eta')$, not from taking the limit. Hence

$$f_1(\eta')\sim(\eta')^{\alpha_1+\alpha_3+1},\quad \alpha_2+\alpha_4<-1\,. \tag{5.14}$$

This shows again that there is an $(\eta')^{\alpha_1+\alpha_3+1}$ branch point.

For $\alpha_2+\alpha_4>-1$, we let $x=x'\eta^{-1}$ and keep only the leading term in the integrand, this being justified by the convergence of the resulting integral. Then

$$\begin{aligned}u &\sim(\lambda_1+\lambda_2+\lambda_3+\lambda_4)x'\eta^{-1}\equiv u_0x'\eta^{-1}\,,\\ v &\sim(\lambda_2+\lambda_4)x'\eta^{-1}\equiv v_0x'\eta^{-1}\,,\end{aligned} \tag{5.15}$$

and

$$f_1(\eta') \sim (\eta')^{\alpha_1-\alpha_2+\alpha_3-\alpha_4} \int_{-\infty}^{\infty} dx' |x'|^{\alpha_2+\alpha_4} e^{iv_0x'} \times M(\alpha_1+1, \alpha_1+\alpha_2+2; -iu_0x') . \tag{5.16}$$

The integral converges at $x'=0$ for $\alpha_2+\alpha_4 > -1$, and therefore

$$f_1(\eta') \sim (\eta')^{\alpha_1-\alpha_2+\alpha_3-\alpha_4}, \quad \alpha_2+\alpha_4 > -1 . \tag{5.17}$$

From Eq. (5.14) and Eq. (5.17) we see that $f_1(\eta')$ has both an $(\eta')^{\alpha_1+\alpha_3}$ term and an $(\eta')^{\alpha_1-\alpha_2+\alpha_3-\alpha_4}$ term.

The analysis of $f_2(\eta')$ is very similar, and the result is

$$\begin{aligned} f(\eta') &\sim (\eta')^0, \quad \alpha_1-\alpha_2+\alpha_3-\alpha_4 > 0 \\ &\sim (\eta')^{\alpha_1-\alpha_2+\alpha_3-\alpha_4}, \quad \alpha_1-\alpha_2+\alpha_3-\alpha_4 < 0 . \end{aligned} \tag{5.18}$$

Hence $f_2(\eta')$ has both an $(\eta')^0$ term and an $(\eta')^{\alpha_1-\alpha_2+\alpha_3-\alpha_4}$ term.

VI. CONCLUSION

We have seen that because of the overlapping cuts in s_1 and s' and because of the complicated Mueller boundary conditions we cannot, in general, express the Regge-cut amplitudes for inclusive reactions in terms of other measurable amplitudes.

In the triple-Regge kinematic region we expect the Regge-cut graphs shown in Fig. 7 to be the most important ones. We can, of course, determine the s and M^2 dependence of the amplitude for each of these graphs. Furthermore, we have noted the following.

(1) We can make a reasonable estimate of the graph shown in Fig. 7(b). The Reggeon-particle vertices have been studied in the analysis of cut contributions to two-body reactions,[19] and the triple-Regge vertex at $k_\perp=0$ can be measured in inclusive reactions.[3] Thus it is only necessary to parametrize the $k_\perp$ dependence of the triple-Regge vertex. We expect that the magnitude of this graph relative to the triple-Regge graph is comparable to the magnitude of Regge cuts relative to Regge poles in two-body reactions.

(2) With a similar parametrization of the nonforward triple-Regge vertices we can estimate the part of the graph in Fig. 7(c) which has the s and M^2 dependence of the graph in Fig. 7(b). We can also calculate the singular part of the contributions of this graph to the four-Reggeon vertex Λ.

(3) We can calculate from measurable triple-Regge couplings the singular part of the contribution of the graph in Fig. 7(d) to Λ.

(4) For arbitrary α_i we can calculate the one-particle contribution to Λ from the double-Regge amplitudes. For special values of the α_i we can determine this contribution from the two-to-three cross section; see Appendix B. Even for these special values of the α_i, however, we cannot, in general, relate Λ to the two-gap cross section[20]: the cuts of the four-Reggeon amplitude in η' are, in general, more complicated than those of the one-particle graphs.

(5) The one-particle approximation for Λ, if it is valid at all, must fail at the points at which it becomes singular.

ACKNOWLEDGMENT

We would like to thank R. D. Field and D. P. Sidhu for useful discussions.

APPENDIX A

Here we work out explicitly the statements made in the Introduction regarding the signs of imaginary parts. First consider the process shown in Fig. 5 and make the replacements

$$p_i \to p_i + i\eta_i , \tag{A1}$$

$$\eta_i^2 = 0, \quad p_i \cdot \eta_i = 0 . \tag{A2}$$

Then

$$\begin{aligned} s &\to s + 2i(\eta_a+\eta_b)\cdot(p_a+p_b) , \\ s_1 &\to s_1 + 2i(\eta_a+\eta_b-\eta_d)\cdot(p_a+p_b-p_d) , \\ s_2 &= s_2 + 2i(\eta_a+\eta_b-\eta_c)\cdot(p_a+p_b-p_c) , \\ s' &= s' + 2i(\eta_a+\eta_b-\eta_c-\eta_d)\cdot(p_a+p_b-p_c-p_d) . \end{aligned} \tag{A3}$$

For large s in the center-of-mass frame we have

$$\begin{aligned} p_a &= \frac{\sqrt{s}}{2}(1001), \quad \eta_a = \epsilon_a(1001) , \\ p_b &= \frac{\sqrt{s}}{2}(100-1), \quad \eta_b = \epsilon_b(100-1) , \\ p_c &= \left(1-\frac{s_2}{s}\right)\frac{\sqrt{s}}{2}(1001) + p_{c\perp}, \quad \eta_c = \epsilon_c(1001) , \\ p_d &= \left(1-\frac{s_1}{s}\right)\frac{\sqrt{s}}{2}(100-1) + p_{d\perp}, \quad \eta_d = \epsilon_d(100-1) , \end{aligned} \tag{A4}$$

assuming s_1, s_2 are also large.

The Mueller graph for the two-particle inclusive reaction requires for ingoing particles

$$\begin{aligned} &(\epsilon_a+\epsilon_b) > 0 , \\ &\epsilon_a\frac{s_1}{s} + (\epsilon_b-\epsilon_d) > 0 , \\ &\epsilon_b\frac{s_2}{s} + (\epsilon_a-\epsilon_c) > 0 , \end{aligned} \tag{A5a}$$

and for outgoing particles

$$(\bar{\epsilon}_a + \bar{\epsilon}_b) < 0 ,$$

$$\bar{\epsilon}_a \frac{s_1}{s} + (\bar{\epsilon}_b - \bar{\epsilon}_d) < 0 , \qquad \text{(A5b)}$$

$$\bar{\epsilon}_b \frac{s_2}{s} + (\bar{\epsilon}_a - \bar{\epsilon}_c) < 0 .$$

Momentum conservation requires

$$\epsilon_a - \epsilon_c = \bar{\epsilon}_a - \bar{\epsilon}_c ,$$
$$\epsilon_b - \epsilon_d = \bar{\epsilon}_b - \bar{\epsilon}_d . \qquad \text{(A6)}$$

So if we put

$$\epsilon_d = \epsilon_b - \delta ,$$
$$\epsilon_c = \epsilon_a - \delta ,$$
$$\bar{\epsilon}_d = \bar{\epsilon}_b - \delta ,$$
$$\bar{\epsilon}_c = \bar{\epsilon}_a - \delta ,$$

with

$$\epsilon_a , \epsilon_b > 0 , \quad \bar{\epsilon}_a , \bar{\epsilon}_b < 0$$

and

$$|\delta| < \epsilon_a \frac{s_1}{s} , \epsilon_b \frac{s_2}{s} , \ldots ,$$

then all of these conditions are satisfied. If $\delta > 0$

$$\mathrm{Im} s' = 2(\epsilon_a - \epsilon_c) \frac{s_1}{s} \sqrt{s} + 2(\epsilon_b - \epsilon_d) \frac{s_2}{s} \sqrt{s}$$

is positive and if $\delta < 0$, Ims′ is negative.

Now consider Fig. 2 and Sudakov parametrize the loop momenta as

$$k = x p_a + y p_b + k_\perp .$$

We then examine various complex values of p_a, p_b, p_c keeping x, y, and $k_\perp$ real. Momentum conservation now requires that

$$\epsilon_a - \epsilon_c = \bar{\epsilon}_a - \bar{\epsilon}_c ,$$

$$\epsilon_b = \bar{\epsilon}_b .$$

The Mueller boundary conditions for the single-particle inclusive process require that

$$\epsilon_a + \epsilon_b > 0 , \ \bar{\epsilon}_a + \epsilon_b < 0 ,$$

while $\mathrm{Im} M^2 > 0$ implies

$$(\epsilon_a - \epsilon_c) + \epsilon_b \frac{s_2}{s} > 0 .$$

At the same time

$$s_1 = (k + p_a)^2 = ys + 2i\sqrt{s}\, y(\epsilon_a + \epsilon_b) ,$$
$$\bar{s}_1 = (\bar{k} + \bar{p}_a)^2 = ys + 2i\sqrt{s}\, y(\bar{\epsilon}_a + \bar{\epsilon}_b) .$$

So the integration contour goes above the right-hand cuts and below the left-hand cuts in s_1 and vice versa for $\bar{s}_1$.

Likewise,

$$s' = (k + p_a - p_c)^2 = ys_2 + 2iy\left[(\epsilon_a - \epsilon_c)\sqrt{s} + \epsilon_b \sqrt{s}\, \frac{s_2}{s}\right]$$

and the imaginary part of s' is correlated with the imaginary part of M^2 in the same way.

Finally, notice that the energy through the right-hand blob is given by

$$(k - p_b)^2 = -xs - 2ix(\epsilon_a + \epsilon_b)\sqrt{s}$$

and so the contours for $N^R_{\lambda',\lambda}$ follow the same path as in the ordinary cut if $\epsilon_a + \epsilon_b > 0$. (Notice that in taking the discontinuity to obtain the cut contribution to the single-particle inclusive distribution, $\epsilon_a + \epsilon_b$ does not change sign and so $N^R_{\lambda',\lambda}$ does not change sign as it does in the cut contribution to the two-particle amplitude.)

APPENDIX B

We want to see in what cases we can determine the one-particle contribution to Λ from the two-to-three cross section. We suppose that there are two double-Regge amplitudes F_{12} and F_{34}, so that the two-to-three cross section is

$$\sigma = \frac{1}{16\pi s^2} |F_{12} + F_{34}|^2 . \qquad \text{(B1)}$$

From Eq. (3.1) we can write

$$F_{12} = \beta_1\beta_2 (s/s_2)^{\alpha_1} (s_2)^{\alpha_2} (e^{-i\pi(\alpha_2 - \nu_2)/2} W_1 + e^{-i\pi(\alpha_1 - \nu_2 - \nu_{12})/2} W_2) ,$$

$$F_{34} = \beta_3\beta_4 (s/s_2)^{\alpha_3} (s_2)^{\alpha_4} (e^{-i\pi(\alpha_4 - \nu_4)/2} W_3 + e^{-i\pi(\alpha_3 - \nu_4 - \nu_{34})/2} W_4) , \qquad \text{(B2)}$$

where the W_i are real. From the energy dependence of σ we can measure

$$\sigma_1 = W_1^2 + 2\cos\tfrac{1}{2}\pi(\alpha_1 - \alpha_2 - \nu_{12})W_1W_2 + W_2^2,$$
$$\sigma_2 = W_3^2 + 2\cos\tfrac{1}{2}\pi(\alpha_3 - \alpha_4 - \nu_{34})W_3W_4 + W_4^2,$$
$$\sigma_3 = \cos\tfrac{1}{2}\pi(\alpha_2 - \alpha_4 - \nu_2 + \nu_4)W_1W_3 + \cos\tfrac{1}{2}\pi(\alpha_1 - \alpha_4 - \nu_2 + \nu_4 - \nu_{12})W_2W_3$$
$$+ \cos\tfrac{1}{2}\pi(\alpha_2 - \alpha_3 - \nu_2 + \nu_4 + \nu_{34})W_1W_4 + \cos\tfrac{1}{2}\pi(\alpha_1 - \alpha_3 - \nu_2 + \nu_4 - \nu_{12} + \nu_{34})W_2W_4. \quad \text{(B3)}$$

Measurement of polarizations of the external particles gives no additional information. We want to calculate

$$\Lambda = W_1W_3 + \frac{1}{\cos\frac{1}{2}\pi(\alpha_1 - \alpha_2 - \nu_{12})}W_2W_3 + \frac{1}{\cos\frac{1}{2}\pi(\alpha_3 - \alpha_4 - \nu_{34})}W_1W_4 + \frac{1}{\cos\frac{1}{2}\pi(\alpha_1 - \alpha_2 + \alpha_3 - \alpha_4 - \nu_{12} - \nu_{34})}W_2W_4. \quad \text{(B4)}$$

We discuss various cases in which this can be done done.

Case I: $\alpha_1 = \alpha_2$, $\alpha_3 = \alpha_4$, $\tau_1 = \tau_2$, $\tau_3 = \tau_4$. This case is trivial. We have

$$\Lambda = (W_1 + W_1)(W_3 + W_4) = \sigma_3. \quad \text{(B5)}$$

Case II: $\alpha_1 = \alpha_4$, $\alpha_2 = \alpha_3$, $\tau_1 = \tau_4$, $\tau_2 = \tau_3$. For $\tau_1 = \tau_2$ we have

$$\Lambda = W_1W_3 + \frac{1}{\cos\frac{1}{2}\pi(\alpha_1 - \alpha_2)}W_2W_3 + \frac{1}{\cos\frac{1}{2}\pi(\alpha_1 - \alpha_2)}W_1W_4 + W_2W_4 = \frac{1}{\cos\frac{1}{2}\pi(\alpha_1 - \alpha_2)}\sigma_3. \quad \text{(B6)}$$

For $\tau_1 = -\tau_2$ we have

$$\Lambda = W_1W_3 + \frac{1}{\sin\frac{1}{2}\pi(\alpha_1 - \alpha_2)}W_2W_3 - \frac{1}{\sin\frac{1}{2}\pi(\alpha_1 - \alpha_2)}W_1W_4 - W_2W_4 = -\frac{1}{\sin\frac{1}{2}\pi(\alpha_1 - \alpha_2)}\sigma_3. \quad \text{(B7)}$$

Case III: $\alpha_3 = \alpha_4 + \nu_{34}$. Then

$$\Lambda = \left[W_1 + \frac{1}{\cos\frac{1}{2}\pi(\alpha_1 - \alpha_2 - \nu_{12})}W_2\right](W_3 + W_4),$$
$$\sigma_1 = W_1^2 + 2\cos\tfrac{1}{2}\pi(\alpha_1 - \alpha_2 - \nu_{12})W_1W_2 + W_2^2,$$
$$\sigma_2 = (W_3 + W_4)^2, \quad \text{(B8)}$$
$$\sigma_3 = [\cos\tfrac{1}{2}\pi(\alpha_2 - \alpha_4 - \nu_2 + \nu_4)W_1 + \cos\tfrac{1}{2}\pi(\alpha_1 - \alpha_4 - \nu_2 + \nu_4 - \nu_{12})W_2](W_3 + W_4).$$

Up to sign ambiguities we can solve for W_1 and W_2 and hence determine Λ.

*Work supported by Energy Research and Development Administration.

[1] A. H. Mueller, Phys. Rev. D 2, 2963 (1970).

[2] M. S. Chen *et al.*, Phys. Rev. Lett. 26, 1585 (1971); E. Beier *et al.*, Univ. of Pennsylvania report, 1974 (unpublished).

[3] R. D. Field and G. C. Fox, Caltech Report No. CALT-68-434, 1974 (unpublished).

[4] H. D. I. Abarbanel and D. J. Gross, Phys. Rev. Lett. 26, 732 (1971).

[5] D. Aschaan *et al.*, in *Proceedings of the XVII International Conference on High Energy Physics, London, 1974,* edited by J. R. Smith (Rutherford Laboratory, Chilton, Didcot, Berkshire, England, 1974).

[6] R. J. N. Phillips, G. A. Ringland, and R. P. Worden, Phys. Lett. 40B, 239 (1972); J. Soffer and D. Wray Nucl. Phys. B73, 231 (1974).

[7] R. D. Field, Caltech Report No. CALT-68-459, 1974 (unpublished).

[8] V. N. Gribov, Zh. Eksp. Teor. Fiz. 53, 654 (1967) [Sov. Phys.—JETP 26, 414 (1968)].

[9] V. N. Gribov and A. A. Migdal, Yad. Fiz. 8, 1002 (1968) [Sov. J. Nucl. Phys. 8, 583 (1969)]; 8, 1128 (1968) [8, 703 (1969)].

[10] I. J. Muzinich, F. E. Paige, T. L. Trueman, and L.-L. Wang, Phys. Rev. D 6, 1048 (1972).

[11] A. B. Kaidalov, Yad. Fiz. 13, 401 (1971) [Sov. J. Nucl. Phys. 13, 226 (1971)].

[12] H. P. Stapp, Phys. Rev. D 3, 3177 (1971); C.-I Tan, *ibid.* 4, 2412 (1971).

[13] V. V. Sudakov, Zh. Eksp. Teor. Fiz. 30, 87 (1956) [Sov. Phys.—JETP 3, 65 (1956)].

[14] M. Toller, Nuovo Cimento 52A, 341 (1969).

[15] P. Hoyer and T. L. Trueman, Phys. Rev. D 10, 921 (1974).

[16] C. E. DeTar, C. E. Jones, F. E. Low, J. H. Weis, J. E. Young, and C.-I Tan, Phys. Rev. Lett. 26, 675 (1971).

[17] H. D. I. Abarbanel and J. B. Bronzan, Phys. Lett. 48B, 345 (1974); Phys. Rev. D 9, 2397 (1974); A. A. Migdal, A. M. Polyakov, and K. A. Ter-Martirosyan, Phys. Lett. 48B, 239 (1974).

[18] V. A. Abramovskii, O. V. Kanchelli, and V. N. Gribov, in *Proceedings of the XVI International Conference on*

High Energy Physics, Chicago-Batavia, Ill., 1972, edited by J. D. Jackson and A. Roberts (NAL, Batavia, Ill., 1973), Vol. 1, p. 389.
[19]S. Frautschi and B. Margolis, Nuovo Cimento 56A, 1155 (1968); F. Henyey, G. Kane, J. Pumplin, and M. Ross, Phys. Rev. 182, 1579 (1969).
[20]C. E. DeTar, Phys. Rev. D 11, 866 (1975).
[21]M. Jacob and G. C. Wick, Ann. Phys. (N.Y.) 7, 404 (1959).
[22]C. E. DeTar and J. H. Weis, Phys. Rev. D 4, 3141 (1971).
[23]I. T. Drummond, P. V. Landshoff, and W. J. Zakrzewski, Nucl. Phys. B11, 383 (1969).
[24]J. H. Weis, Phys. Rev. D 6, 2823 (1972).
[25]F. E. Paige, T. L. Trueman, and L.-L. Wang (unpublished).
[26]S. J. Chang, D. Gordon, F. E. Low, and S. B. Treiman, Phys. Rev. D 4, 3055 (1971); A. H. Mueller and T. L. Trueman, *ibid.* 5, 2115 (1972).
[27]J. H. Schwarz, Phys. Rev. 162, 1671 (1967).
[28]G. Veneziano, Nuovo Cimento 57A, 190 (1968); K. Bardakci and H. Ruegg, Phys. Rev. 181, 1884 (1969); H. M. Chan and S. T. Tsou, Phys. Lett. 28B, 485 (1969); C. G. Goebel and B. Sakita, Phys. Rev. Lett. 22, 257 (1969); Z. Koba and H. B. Nielsen, Nucl. Phys. B10, 633 (1969); B12, 517 (1969).
[29]*Handbook of Mathematical Functions,* edited by M. Abramowitz and I. A. Stegun (National Bureau of Standards, Washington, 1966), Chap. 13.